

# Taipan: A Query-free Transfer-based Multiple Sensitive Attribute Inference Attack Solely from Publicly Released Graphs

Ying Song and Balaji Palanisamy  
*University of Pittsburgh  
 Pittsburgh, PA, USA*

## Abstract

Graph-structured data underpin a wide spectrum of modern applications. However, complex graph topologies and homophilic patterns can facilitate attribute inference attacks (AIAs) by enabling sensitive information leakage to propagate across local neighborhoods. Existing AIAs predominantly assume that adversaries can probe sensitive attributes through repeated model queries. Such assumptions are often impractical in real-world settings due to stringent data protection regulations, prohibitive query budgets, and heightened detection risks, especially when inferring multiple sensitive attributes. More critically, this model-centric perspective obscures a pervasive blind spot: **intrinsic multiple sensitive information leakage arising solely from publicly released graphs**. To exploit this unexplored vulnerability, we introduce a new attack paradigm and propose **Taipan**, the first query-free transfer-based attack framework for multiple sensitive attribute inference attacks on graphs (G-MSAIAs). Taipan integrates *Hierarchical Attack Knowledge Routing* to capture intricate inter-attribute correlations, and *Prompt-guided Attack Prototype Refinement* to mitigate negative transfer and performance degradation. We further present a systematic evaluation framework tailored to G-MSAIAs. Extensive experiments on diverse real-world graph datasets demonstrate that Taipan consistently achieves strong attack performance across same-distribution settings and heterogeneous similar-and out-of-distribution settings with mismatched feature dimensionalities, and remains effective even under rigorous differential privacy guarantees. Our findings underscore the urgent need for more robust multi-attribute privacy-preserving graph publishing methods and data-sharing practices.

## 1 Introduction

The rapid proliferation of machine learning (ML) techniques has transformed data into a cornerstone of the global digital economy, driving breakthroughs in large language models [33] and autonomous driving [39], while revitalizing traditional fields such as financial management and marketing.

However, data abundance has also triggered unprecedented privacy concerns. As research institutions, private enterprises, and government sectors increasingly leverage proprietary datasets for model training, sensitive information is disseminated across complex ML pipelines, substantially expanding the surface for privacy leakage. These risks are further amplified when trained models are publicly accessible, either through released model parameters or inference APIs. Even under restricted access, prior studies have shown that ML models remain vulnerable to attribute inference attacks (AIAs) [11, 13, 22], which enable adversaries to recover sensitive attributes of training records through model queries. Furthermore, most real-world data are relational and can be naturally modeled as homophilic graphs, where entities sharing similar sensitive attributes tend to associate with others [9]. As a result, the disclosure of one entity’s sensitive attributes can propagate privacy risks to its associated neighbors. Recent research also confirms that graph neural networks (GNNs), which are tailored for graph-structured data, can amplify privacy leakage by aggregating and propagating sensitive information through message passing [12, 25]. This amplification can lead to severe social consequences, particularly in high-stakes domains. For instance, attackers may launch AIAs to infer the health status, education level, or crime history of targeted individuals and their associated neighbors in financial credit networks. Such unauthorized inference facilitates surveillance, blackmail, and identity theft, thereby undermining the security and trustworthiness of financial systems.

The effectiveness of existing query-based AIAs fundamentally relies on adversaries’ abilities to repeatedly probe the victim model. While successful in controlled settings, such attacks are still constrained in practice by strict query budgets and increasingly robust defenses. Moreover, they only target a single sensitive attribute and fail to generalize to arbitrary records with multiple sensitive attributes. In this work, we move beyond model-dependent leakage and adopt a data-driven perspective to reveal an inherent vulnerability that arises solely from publicly released graphs. Accordingly, we propose a new transfer-based paradigm for multiple sensitive

AIAs on graphs (G-MSAIAs) in a query-free manner. Unlike traditional AIAs, transfer-based MSAIAs substantially lower the attack barriers and leave no interaction footprint on victim models, making them difficult to trace and detect. Since current defense mechanisms primarily focus on model-centric safeguards to circumscribe adversaries’ capabilities, they are ineffective against the persistent and pervasive privacy leakage originating from the ubiquity of open-source graphs and those readily obtained through web-scraping or data breaches.

**Limitations of Prior Work** To the best of our knowledge, the investigation on AIAs in the graph domain remains in its infancy. Existing AIAs either utilize node embeddings together with auxiliary graphs to train supervised attack models [12], or operate as data imputation methods to infer missing sensitive attributes values given the remaining records [25]. Beyond the graph domain, AIAs predominantly adopt a query-based paradigm. The key idea behind these attacks is that victim models tend to produce more confident posterior probabilities or more accurate predictions when queried with the true sensitive attribute value of a target record [22]. This paradigm implicitly assumes that sensitive attributes are retained during model training and can be exposed through repeated probing. Despite its effectiveness in black-box settings, this assumption breaks down in real-world applications for two primary reasons. First, to comply with data protection regulations such as the General Data Protection Regulation (GDPR) [16], model owners are required to sanitize sensitive attributes prior to training and to mitigate sensitive information leakage through privacy-preserving mechanisms during or after model training. As a result, sensitive attributes can no longer be feasibly exposed through this paradigm. Second, repeated queries generate anomalous access patterns that are easily detected by anomaly detection systems. Additionally, such attacks incur prohibitive query budgets when dealing with sensitive attributes with multiple categorical values.

Existing AIAs are also limited in their applicability. They typically focus on inferring sensitive attributes of a small subset of training records and exhibit poor generalization to non-training ones. While imputation-based attacks may succeed when training and non-training records follow the same or highly similar distributions, their effectiveness degrades substantially when confronted with out-of-distribution (OOD) records. In addition, most existing studies target a single sensitive attribute, and only a few works consider multi-attribute leakage in tabular data. However, they adopt simplistic extensions, either conducting the same AIA for each attribute in parallel [18] or sequentially [22], and are therefore only applicable to small-scale training datasets with a limited number of sensitive attributes. Most importantly, these AIAs cannot be trivially extended to graphs, where multiple sensitive attributes are often intertwined and exhibit complex pairwise correlations induced by topological dependencies and homophilic patterns.

**Research Questions** The aforementioned research gap moti-

vates us to investigate the following three research questions:

1. *Is it possible to design a unified attack framework that can jointly infer multiple sensitive attributes on graphs?*
2. *Can this framework generalize to the OOD setting while remaining effective under strong privacy guarantees?*
3. *How can we systematically evaluate the attack performance of G-MSAIAs?*

**Challenges** We identify five key challenges to address the above research questions.

1. “Information Vacuum”: Without query responses as informative proxies, even conducting a query-free AIA for a single sensitive attribute on unseen graphs becomes highly challenging. This difficulty is further exacerbated when simultaneously inferring multiple sensitive attributes.
2. Intertwined Correlations: Multiple sensitive attributes often exhibit intricate correlations driven by demographic, cultural, or historical factors. Hence, training a unified attack model is challenging, as easily inferred attributes may dominate the learning process while overshadowing the nuanced patterns of underrepresented attributes. Furthermore, conflicting or negatively correlated sensitive attributes can distort the shared latent space and ultimately degrade the overall inference accuracy.
3. Out-of-distribution (OOD) Records: OOD records introduce distributional shifts that are amplified under multi-attribute attack settings, leading to negative transfer and degraded attack performance.
4. Privacy Guarantees: In practice, graphs are often published under strong privacy guarantees, which further amplify the misalignment between auxiliary and target graphs.
5. Comprehensive Evaluation: Existing AIA evaluation metrics are tailored for a single sensitive attribute and cannot be trivially extended to G-MSAIAs.

**Solutions and Contributions** We propose a query-free data-only transfer-based multiple sensitive attribute inference attack framework named **Taipan**. This unified framework comprises two core modules: *Hierarchical Attack Knowledge Routing* and *Prompt-guided Attack Prototype Refinement*. Inspired by multi-task learning (MTL), we formulate the inference of each sensitive attribute as an individual attack task. Unlike traditional shared-bottom MTL architectures, we build upon the Multi-gate Mixture-of-Experts (MMoE) framework [21] to flexibly capture intricate inter-attribute correlations while suppressing task interference and performance degradation. Specifically, we first profile attack tasks on the auxiliary graph and construct an attack hierarchy tree. Guided by this hierarchy, we design a hierarchical MMoE-based architecture that promotes positive transfer among similar attack

tasks while mitigating negative transfer among conflicting tasks. To capture both shared and task-specific knowledge, we introduce learnable pretext tokens as task identifiers [37]. During transfer, we freeze the pre-trained Taipan and only tune the lightweight pretext token parameters, which act as prompts to extract structural and semantic knowledge from the auxiliary graph and adapt it to the target graph. Since we strictly assume that sensitive attributes in the target graph are masked or sanitized under rigorous privacy safeguards, this realistic setting naturally formulates attack transfer as an unsupervised domain adaptation problem, where the attack model should align knowledge learned from the auxiliary graph with sparse or distorted signals in the target graph. We initially employ pseudo labeling using the pre-trained Taipan and only preserve high-confidence nodes and then reuse auxiliary samples during adaptation to further alleviate data scarcity. Additionally, we adaptively adjust attack prototypes to exploit the rich information from filtered target nodes, enabling smooth and reliable distribution alignment. Finally, for comprehensive evaluation, we introduce three categories of metrics to systematically assess attack utility, task deviation, and semantic knowledge preservation, respectively.

To the best of our knowledge, no unified graph MMoE (GMMoE) framework exists for general graph learning, and existing efforts are limited to a few GNN applications [5, 14, 41]. Furthermore, no prior work has investigated multi-task prompt tuning for unsupervised graph domain adaptation. We design the first GMMoE-based framework to handle complex interdependencies across multiple node-level tasks, together with the first prompting mechanism for transferring multi-task knowledge from a well-structured source graph to an ill-distributed target graph. Notably, we distinguish between conventional “attack transferability” and our proposed “attack transfer”. The former refers to reusing adversarial examples across models, whereas the latter denotes transferring attack knowledge from a pre-trained attack model to downstream attack tasks. This notion resembles standard transfer learning, but serves for malicious purposes. To our knowledge, this is the first study to investigate attack transfer in the graph domain, and even in general tabular settings.

**Summary:** In summary, our contributions include:

1. We propose a new attack paradigm for G-MSAIAs, and design the first query-free transfer-based attack framework with two novel modules for multi-attribute inference.
2. We pioneer the investigation of multiple “attack transfer” using only publicly released graphs.
3. We introduce a comprehensive and systematic evaluation framework to quantify G-MSAIAs.
4. Extensive experiments demonstrate the effectiveness and efficiency of Taipan under diverse distribution settings.
5. Our empirical results show that Taipan remains effective under strong privacy guarantees, highlighting an urgent

need for more robust multi-attribute privacy-preserving graph publishing methods and for a re-evaluation of data-sharing practices and regulatory policies, as privacy harm can occur without explicit data misuse or model abuse.

## 2 Background and Related Work

### 2.1 Notations

Given an undirected attributed graph  $\mathcal{G} = (\mathcal{V}, \mathcal{E}, \mathcal{X})$ ,  $\mathcal{V}$  denotes the node set with  $|\mathcal{V}|$  nodes, and  $\mathcal{E} \subseteq \mathcal{V} \times \mathcal{V}$  denotes the edge set with  $|\mathcal{E}|$  edges. The graph topology is represented by the adjacency matrix  $\mathcal{A} \in \mathbb{R}^{|\mathcal{V}| \times |\mathcal{V}|}$ , where  $\mathcal{A}_{u,v} = 1$  if and only if the edge  $(u, v) \in \mathcal{E}$ , otherwise  $\mathcal{A}_{u,v} = 0$ . Each node  $v \in \mathcal{V}$  is associated with a feature vector  $\mathcal{X}_v = \{\mathcal{S}_v, \mathcal{X}_v\} \in \mathbb{R}^d$  and a label  $\mathcal{Y}_v$ , where  $\mathcal{S}_v$  denotes sensitive attributes (e.g., gender, age, and marriage status),  $\mathcal{X}$  denotes non-sensitive attributes, and  $d$  represents the feature dimensionality.

### 2.2 Graph Neural Networks

Generally, GNNs aggregate information for each node  $v \in \mathcal{V}$  from its local neighborhood  $\mathcal{N}(v)$  and iteratively update its representation  $Z_v$ . This message passing process can be formulated as:

$$Z_v^L = \text{UPD}^L(Z_v^{L-1}, \text{AGG}^{L-1}(\{Z_u^{L-1} : u \in \mathcal{N}(v)\})) \quad (1)$$

where  $L$  denotes the number of GNN layers and  $Z_v^0 = \mathcal{X}_v$  represents the initial feature vector of node  $v$ . The operators  $\text{UPD}$  and  $\text{AGG}$  are differentiable aggregation and update functions, respectively, which can be instantiated to construct various GNN architectures. For node classification tasks, the final node embedding  $Z_v^L$  is mapped to the predicted label  $\hat{\mathcal{Y}}_v$  through a linear classifier  $f_\theta(\cdot)$  followed by a softmax function, where  $\theta$  denotes the trainable parameters of the classification head.

### 2.3 Attribute Inference Attack

#### 2.3.1 Attribute Inference Attacks on Tabular Data

FJRMIA [13] establishes the foundation paradigm for AIAs by repeatedly querying a victim model with perturbed sensitive attribute values and identifying the value that yields the highest posterior probability. Building upon this paradigm, CSMIA [22] removes the reliance on confusion matrices or marginal priors. For a target record in the training dataset, CSMIA queries the victim model with all possible sensitive attribute values while keeping non-sensitive attributes fixed, and selects the value that maximizes the model’s confidence score when the prediction is correct. Unlike CSMIA, LOMIA supports label-only queries. It constructs an attack dataset by querying the victim model with all possible sensitive attribute values of a target record and retaining only those queries that

Table 1: **Attack Comparison.**  $\checkmark$  represents “access” or “applicable”,  $\times$  represents “no access” or “not applicable”.  
 Dist.:Distribution; Impt.: Imputation; SA: Sensitive Attribute; Sim.: Similar; Diff.: Different.

Attack Name	Attack Target			Attack Participant		Attack Knowledge and Adversary’s Capabilities			Attack Mechanism
	Phase	Type	Inference	Model Owner	Attacker	Data Access	Model Access	Model Outputs	
FJRMIA [13]	Training	Tabular	Single	$\checkmark$	$\checkmark$	Full Non-SAs in Training Data Marginal Prior of SAs and Non-SAs Possible Values of SAs and Non-SAs Training Data’s Ground-truth Labels	Black Box	Confusion Matrix Confidence Score	Query-based, Posterior-maximized
CS/LOMIA [22]	Training	Tabular	Single Parallel	$\checkmark$	$\checkmark$	Full Non-SAs in Training Data Possible Values of SAs and Non-SAs Training Data’s Ground-truth Labels (Auxiliary Data with Same/Similar Dist.)	Black Box	Confidence Score (Label-only)	Query-based, Posterior-maximized (Attack Model Trained)
Sens. Val. Inf. [17]	Training	Tabular	Single	$\checkmark$	$\checkmark$	Full Non-SAs in Training Data Possible Values of SAs and Non-SAs Auxiliary Graph with Same/Similar Dist. and Similar Shadow Model	White/Black	Confidence Score	Neuron Impt.-exploited Query-based
SDMIA [11]	Training	Tabular	Single	$\checkmark$	$\checkmark$	Possible Values of SAs and Non-SAs	Black Box	Label-only	Query-based, Attack Model Trained
Disparity Inf. [18]	Training	Tabular	Single/ Sequential	$\checkmark$	$\checkmark$	Full Non-SAs in Training Data Possible Values of SAs and Non-SAs	Black Box	Confidence Score	Query-based, Disparity-exploited
Duddu et al. [12]	Training	Graph	Single	$\checkmark$	$\checkmark$	Auxiliary Graph with the Similar Dist. Node Embeddings of All Graphs	Grey Box	Node Embeddings	Query-based, Attack Model Trained
FP&FP-MA [25]	Training	Graph	Single/ Missing	$\checkmark$	$\checkmark$	Full Non-SAs and Partial SAs Auxiliary Graph with Same/Similar Dist. and Similar Shadow Model	Black Box	Confidence Score	Query-based, Posterior-maximized
G-MSAIA (Ours)	All	Graph	Multiple	$\times$	$\checkmark$	Auxiliary Graph with Same/Sim./Diff. Dist. Possible Values of SAs	$\times$	$\times$	Transfer-based, Data-driven

yield correct predictions. These correctly classified records are then used to train an attack model that exploits correlations between sensitive and non-sensitive attributes. Although both CSMIA and LOMIA can be extended to infer multiple sensitive attributes, such extensions simply repeat single-attribute inference in parallel, thereby incurring prohibitive query budgets and high detection risks. Jayaraman et al. [17] propose a sensitive value inference attack under the white-box setting, where auxiliary data are utilized to identify neurons that are most correlated with sensitive attributes. For each target record, adversaries infer the sensitive value if the weighted sum of the activations of these neurons exceeds a pre-specified threshold. SDMIA [11] assumes only minimal knowledge of the possible values of sensitive and non-sensitive attributes and employs random queries to construct an attack dataset by retaining instances whose predictions differ across all candidate sensitive values. Recently, Kabir et al. [18] identify disparate vulnerability across demographic subgroups by analyzing angular differences in confidence score distributions, and exploit such disparities to conduct AIAs targeting the most vulnerable records. While this disparity-based approach can be extended to multiple sensitive attributes, it infers them sequentially, resulting in prohibitively high query budgets.

### 2.3.2 Attribute Inference Attack against GNNs

AIAs against GNNs remain relatively underexplored. Duddu et al. [12] propose the first AIA framework against GNNs, which assumes that adversaries can obtain node embeddings of an auxiliary graph together with their corresponding sensitive attributes. However, this assumption is unrealistic in real-world deployments due to stringent security and privacy regulations that restrict access to internal model representa-

tions. FP and FP-MA [25] exploit the feature propagation mechanism inherent in GNNs to perform AIAs, but they are fundamentally data imputation methods that recover partially missing sensitive attributes rather than jointly inferring multiple sensitive attributes.

For clarity, we summarize these representative AIAs in Table 1. Overall, no unified attack framework currently exists for simultaneously inferring multiple sensitive attributes. Existing extensions either simply repeat single-attribute inference in parallel or sequentially, or rely on data imputation methods, which are insufficient to address the challenges posed by complex graph-structured data.

## 3 Attack Framework Design

In this section, we formalize the threat model and present Taipan, the first query-free, transfer-based attack framework for multiple sensitive attribute inference on graphs.

### 3.1 Threat Model

#### 3.1.1 Adversary’s Goal

The adversary’s objective is to simultaneously infer multiple sensitive attributes on a target graph in a query-free manner, without interacting with any victim models. We formally define the attack model and transfer mechanism below.

**Definition 1** (*Multiple Sensitive Attribute Inference Attacks on Graphs (G-MSAIAs)*): Given a target graph  $\mathcal{G}_t$ , sensitive attributes  $\mathcal{S}_t \in \mathbb{R}^{|\mathcal{V}_t| \times s}$  are masked due to privacy concerns, and only non-sensitive attributes  $\mathcal{X}_t \in \mathbb{R}^{|\mathcal{V}_t| \times (d-s)}$ , which may additionally be processed by privacy-preserving techniques,

are publicly available, where  $s$  denotes the number of sensitive attributes. The adversary aims to construct an attack model  $\mathcal{F}$  to infer the sensitive attributes of a subset of target nodes  $\mathcal{V}_t^m \in \mathcal{V}_t$ , where typically  $m = |\mathcal{V}_t|$ .

**Definition 2 (Attack Transfer Mechanism):** Given a target graph  $\mathcal{G}_t = (\mathcal{V}_t, \mathcal{E}_t, \mathcal{X}_t)$  without access to sensitive labels  $\mathcal{S}_t$  and a publicly available graph  $\mathcal{G}_a$  with sensitive labels  $\mathcal{S}_a$ , the adversary first pre-trains an attack model  $\mathcal{F}_{pre}(\mathcal{G}_a, \mathcal{S}_a)$ , and then adapts it to the unlabeled target graph  $\mathcal{G}_t$  to obtain a tuned attack model  $\mathcal{F}_{tun}(\mathcal{G}_t)$ , which is used to infer the sensitive attributes  $\mathcal{S}_t^m$  of target nodes  $\mathcal{V}_t^m$  in  $\mathcal{G}_t$ .

### 3.1.2 Adversary’s Knowledge and Capabilities

We consider a data-only, query-free threat model, where the adversary has no access to victim GNNs, including their model parameters, training procedures, internal representations, or query interfaces. Instead, the adversary extracts sensitive signals solely from the intrinsic structural and semantic properties of publicly available graphs.

This attack model fundamentally differs from that of conventional AIAs, which typically assume that adversaries can manipulate sensitive attributes and repeatedly query victim models to probe their real values. However, such assumptions can be misaligned with practical deployment settings for two main reasons. First, to comply with stringent data protection regulations such as the General Data Protection Regulation (GDPR) [16], sensitive attributes are commonly masked and sensitive correlations are mitigated prior to model training, rendering attacks that rely on manipulating sensitive attributes ineffective. Second, repeated queries are often constrained by access controls, rate limiting, and model or system monitoring mechanisms, which restricts the feasibility of query-based attacks. Moreover, even under strong attack capabilities and rich prior knowledge, recent studies [17, 18] show that such attacks struggle to achieve consistently high attack performance. In contrast, numerous graph datasets are widely released for research or commercial purposes, or can be easily collected through web scraping and data-sharing agreements. Such datasets can serve as auxiliary data for data-only G-MSAIAs without reliance on victim models.

Following standard assumptions in prior AIAs [11, 17, 18, 22, 25], we assume that the possible values of multiple sensitive attributes (e.g., female/male for gender) in the target graph are known to the adversary. We further assume that the adversary initially has access only to non-sensitive attributes in the target graph. Since privacy-preserving techniques are often imposed during graph publishing, we additionally evaluate our attack under a rigorous privacy regime, namely differential privacy [42], as detailed in Section 4.4.1.

### 3.1.3 Attack Scenarios

We consider three attack scenarios based on the availability and alignment of auxiliary graphs with the target graph. These scenarios do not alter the adversary’s capabilities defined in the threat model, but are used to demonstrate the feasibility and generality of the proposed attack under progressively relaxed assumptions on auxiliary data availability.

**Same-Distribution Auxiliary Graph.** Following common practice in prior inference attacks, we first consider an idealized setting where the auxiliary graph is drawn from the same underlying distribution as the target graph.

**Out-of-distribution (OOD) Auxiliary Graph.** We then relax the assumption and consider auxiliary graphs originating from the same application domain but collected from different data sources. Such auxiliary graphs are generally more accessible than same-distribution data and naturally exhibit distribution shifts in graph topology as well as heterogeneous feature spaces with mismatched dimensionalities.

**Task-Shifted Auxiliary Graph.** We further relax the assumption and consider auxiliary graphs drawn from the same broad application domain as the target graph. In this resource-constrained scenario, auxiliary graphs are associated with related but distinct prediction tasks and exhibit heterogeneous structural and feature representations. Such auxiliary data serve as a fallback when moderately aligned auxiliary graphs are scarce. For instance, the target graph may represent a social network such as Facebook for modeling social communities, while the auxiliary graph is derived from LinkedIn to capture professional relationships. Although both graphs belong to the same broad domain and share overlapping multiple sensitive attributes, e.g., basic demographic information, they exhibit substantial task and distributional shifts.

Taken together, these scenarios demonstrate that the proposed attack can succeed under a wide range of auxiliary data conditions, including weakly aligned and heterogeneous settings. Moreover, since group disparities can be exploited by adversaries to conduct AIAs [18], such attacks may also serve as a tool for privacy auditing of fairness techniques [1], particularly in high-stakes applications.

## 3.2 Framework Design

In this section, we introduce Taipan, the first attack framework for G-MSAIAs and provide its overview in Figure 1. We then present a systematic evaluation framework to measure multiple sensitive information leakage.

### 3.2.1 Design Rationale

G-MSAIAs aim to simultaneously infer multiple sensitive attributes, which naturally aligns with a graph multi-task learning (GMLT) paradigm. This paradigm exploits shared and complementary information among multiple related tasks to

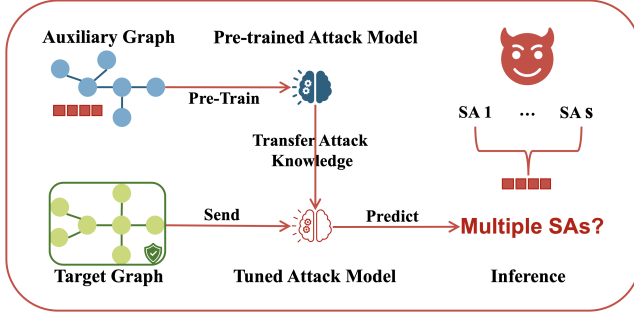


Figure 1: The Framework Overview of Taipan for G-MSAIAs. The stacked squares represent multiple sensitive attributes and the green shield indicates the privacy-preserving techniques.

guarantee or even improve performance through multitask synergy while reducing computational and storage costs [36].

Under the realistic query-free and data-only attack setting, G-MSAIAs can be reformulated as a “multi-task attack transfer” problem, where adversaries leverage an auxiliary graph to infer multiple sensitive attributes on a target graph without interacting with any victim models. Although all attack tasks share the same auxiliary graph as prior knowledge and rely on the same target-graph topology and non-sensitive attributes as observable signals, they may differ substantially in semantics and prediction difficulty. Moreover, in practice, correlations among sensitive attributes can be positive, negative, or negligible, leading to complex and sometimes conflicting optimization dynamics.

As a result, constructing a unified attack model for all attack tasks is inherently challenging: dominant tasks may overwhelm the optimization process, while conflicting tasks can induce gradient interference, causing optimization difficulty, slower convergence, and poor performance on weakly-related tasks or even across all tasks. Additionally, to comply with security and privacy regulations, sensitive attributes are typically removed prior to graph publishing and model training. Consequently, adversaries have no access to sensitive labels in the target graph and must infer multiple sensitive attributes from weak, indirect or even distorted signals alone, which further exacerbates the difficulty of query-free G-MSAIAs.

These challenges call for an attack framework that can flexibly balance shared and task-specific attack knowledge, explicitly model diverse task correlations, and remain parameter-efficient under realistic query-free and data-only settings. The Multi-gate Mixture-of-Experts (MMoE [21]) paradigm has emerged as a promising solution for flexibly handling complex task correlations while mitigating model collapse and performance degradation. It constructs a suite of shared expert networks to handle multiple tasks and utilizes a task-specific multi-gate mechanism to dynamically modulate these experts by assigning different weights. This parameter-efficient architecture substantially reduces the cumulative computa-

tional costs and storage requirements compared to independent single-task training. Nonetheless, MMoE cannot be trivially adapted to G-MSAIAs for several reasons. First, to the best of our knowledge, no unified graph MMoE framework exists. Since graphs exhibit complex topological structures and rich node features, existing MMoE frameworks tailored for tabular data cannot be directly extended to graphs. Second, G-MSAIAs necessitate transferring attack knowledge from a labeled auxiliary graph to an unlabeled target graph, which may follow a different distribution from the target graph under realistic attack settings. However, classical MMoE frameworks cannot address such unsupervised heterogeneous domain adaptation. Third, despite its parameter efficiency, naively fine-tuning a pre-trained MMoE attack model incurs additional computational and storage overheads that are not feasible in low-resource attack scenarios. In addition, updating all parameters might corrupt the general attack knowledge, leading to poor adaptation and generalization.

To address the above challenges, we propose Taipan, a novel attack framework for G-MSAIAs. Taipan consists of two core modules: *Hierarchical Attack Knowledge Routing* and *Prompt-guided Attack Prototype Refinement*. We detail the design of Taipan in the following sections.

### 3.2.2 Hierarchical Attack Knowledge Routing

*Hierarchical Attack Knowledge Routing* is designed to adaptively route shared and task-specific attack signals within a unified pre-trained model, enabling each inference task to extract transferable knowledge while mitigating negative interference among multiple sensitive attributes. It involves two stages: (1) profiling attack tasks to characterize and exploit diverse sensitive correlations; (2) assigning task identifiers to support task-aware attack knowledge routing and downstream sensitive attribute inference.

**Attack Profiling** G-MSAIAs first require profiling the complex correlations among multiple attack tasks. Existing MTL frameworks typically quantify such correlations either through the inter-task similarity of task gradients on shared prompts [20] or via learnable task covariance matrices [36]. Despite their success, these approaches often incur high optimization difficulty and substantial computational overhead. To alleviate this issue, we adopt a simple yet effective strategy. Specifically, we compute pairwise cosine similarities among sensitive attributes in the auxiliary graph and then apply agglomerative hierarchical clustering [10] on their inter-similarity matrix to profile attack tasks. This profiling produces an attack hierarchy that captures fine-grained shared attack signals, enabling positive transfer among similar tasks while mitigating negative transfer among conflicting tasks.

Guided by the attack hierarchy, we construct an MMoE-based multi-task attack framework composed of a suite of expert networks, gating networks, and task heads, as shown in Figure 2. The framework governs how experts are shared and

how gates route attack knowledge across hierarchical clusters and inference tasks. When sensitive attributes exhibit no meaningful correlations, the hierarchy becomes uninformative, and the framework naturally degenerates to a flat multi-task architecture with a shared expert alongside task-specific experts, gates, and heads.

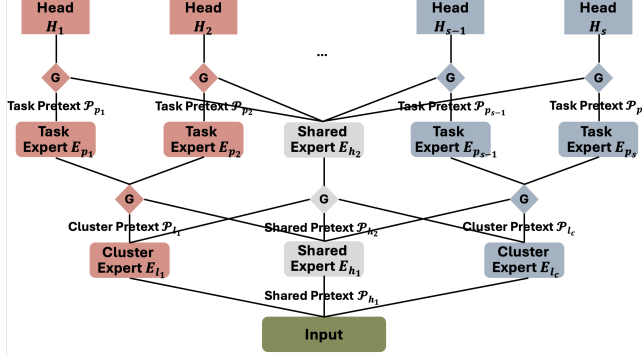


Figure 2: Hierarchical Attack Knowledge Routing

**Task Identifier Assignment** The primary objective of the framework is to extract both shared and task-specific attack knowledge to assist downstream attribute inference. While the attack hierarchy alleviates negative transfer among conflicting tasks, the shared encoder may still struggle to disentangle fine-grained, task-specific semantics from global shared representations when routing experts across different tasks. We therefore introduce attack task identifiers to enable more task-aware attack knowledge routing.

Inspired by MULTIGPrompt [37], we instantiate attack task identifiers using pretext tokens, which are learnable vectors that can be injected into the pre-training graph [28, 29] or integrated into the GNN architecture [37]. Unlike MULTIGPrompt, which employs composite pretext tokens to modulate the input, hidden, and output layers of a shared encoder, we assign pretext tokens to each expert of the attack hierarchy to explicitly construct a hierarchical attack path. This design enables pretext tokens to function as task instructions that guide both shared and task-specific attack knowledge extraction, while inducing well-structured computational pathways tailored to different inference tasks. As a result, hierarchical task-aware routing effectively reduces gradient interference and mitigates negative transfer, while enhancing transferability and robustness across multiple attack tasks. In addition, pretext tokens serve as controllable semantic anchors, facilitating efficient and reliable adaptation to downstream sensitive attribute inference.

Formally, given a full hierarchical attack path which integrates an attack hierarchy  $\mathcal{T}$  with  $\kappa$  hierarchy and  $c$  clusters (for clarity of illustration, we omit subclusters, i.e.,  $\kappa = 2$ . Extensions to deeper hierarchies are straightforward), we instantiate three types of experts—shared experts  $E_h$ , cluster-shared experts  $E_l$  and task-specific experts  $E_p$ —and place them at

their corresponding levels in the path. Each expert is paired with a corresponding gating network, denoted by  $G_h$ ,  $G_l$ , and  $G_p$ , together with task-specific heads  $H$ . We further initialize a pretext token set  $\mathcal{P} = \{\mathcal{P}_h, \mathcal{P}_l, \mathcal{P}_p\}$  and attach them to their respective expert along the path, as illustrated in Figure 2. The output of each attack task  $\mathcal{S}_{ai}, i \in \{1, 2, \dots, s\}$  can be formulated as follows:

$$\begin{aligned}
 \mathcal{G}_a^* &= (\mathcal{V}_a, \mathcal{E}_a, X_a^* \odot \mathcal{P}_{h1}) \\
 \mathcal{Z}_{Cj} &= G_{lj}(\mathcal{G}_a^*)^T \{E_{h1}(\mathcal{G}_a^*) \odot \mathcal{P}_{h2}, E_{l1}(\mathcal{G}_a^*) \odot \mathcal{P}_{l1}, \\
 &\quad \dots, E_{lc}(\mathcal{G}_a^*) \odot \mathcal{P}_{lc}\} \\
 \mathcal{Z}_{h1} &= G_h(\mathcal{G}_a^*)^T \{E_{h1}(\mathcal{G}_a^*) \odot \mathcal{P}_{h2}, E_{l1}(\mathcal{G}_a^*) \odot \mathcal{P}_{l1}, \\
 &\quad \dots, E_{lc}(\mathcal{G}_a^*) \odot \mathcal{P}_{lc}\} \\
 \mathcal{Z}_{S_{ai}} &= G_{pi}(\mathcal{Z}_{Cj})^T \{E_{pi}(\mathcal{Z}_{Cj}) \odot \mathcal{P}_{pi}, E_{h2}(\mathcal{Z}_{h1})\} \\
 \hat{\mathcal{S}}_{ai} &= H_i(\mathcal{Z}_{S_{ai}}) \tag{2}
 \end{aligned}$$

where  $C_j$  denotes a cluster in  $\mathcal{T}$ ,  $j \in \{1, 2, \dots, c\}$  and there exists a valid path from  $C_j$  to  $S_{ai}$ .  $\mathcal{P}_h$  represents shared pretext tokens, and the remaining tokens are defined analogously. Each expert network  $E = GNN(\cdot)$  is a GNN encoder, each gating network  $G = \text{softmax}(\sigma(MLP(\cdot)))$  is a 2-layer MLP, and each task head  $H = MLP(\sigma(\cdot))$  is a 1-layer MLP, where  $\sigma$  is a specified activation function, such as ELU [8]. Since auxiliary node labels  $\mathcal{Y}_a$  also contain informative signals, we augment the non-sensitive node features as  $X_a^* = X_a \oplus \mathcal{Y}_a$ .

Finally, the entire framework is optimized by:

$$\mathcal{L}_{att} = \sum_{i=1}^s w_i \cdot l(\mathcal{S}_{ai}, \hat{\mathcal{S}}_{ai}) \tag{3}$$

where  $l(\cdot)$  denotes the attack loss (e.g., cross-entropy). The task weight  $w_i = dCor(\mathcal{S}_{ai}, X_a^* \oplus (\mathcal{S}_a \setminus \mathcal{S}_{ai}))$  is measured by the distance correlation ( $dCor$ ) [30] between each sensitive attribute and the remaining node features. We choose  $dCor$  because it measures statistical dependence in arbitrary dimensions without exhaustive pairwise feature comparisons.

### 3.2.3 Prompt-guided Attack Prototype Refinement

During attack transfer, we first freeze the pre-trained attack model and adapt it to the target graph by only tuning lightweight pretext token parameters. These pretext tokens act as graph prompts, substantially reducing computational overhead while mitigating task interference and negative transfer. Notably, this graph prompting fundamentally differs from the existing node-level reformulation methods that inject learnable vectors or subgraphs into pre-training graphs [6, 28, 29]. Since the target graph is unlabeled, downstream G-MSAIAs can be naturally formulated as an unsupervised domain adaptation (UDA) problem. However, prior multi-task prompt tuning frameworks are primarily designed for supervised domain adaptation [4, 20, 24, 36, 37], leaving multi-task unsupervised domain adaptation largely unexplored, particularly in the graph domain. Additionally, existing unsupervised domain

adaptation methods [3, 7] tailored for tabular data cannot be trivially extended to multi-task graph prompting. Motivated by these limitations, we propose a simple yet effective multi-task prompt tuning attack framework for unsupervised graph domain adaptation. The framework comprises two submodules: *High-confidence Tuning* to mitigate data scarcity and catastrophic forgetting, and *Adaptive Prototype Adjustment* to adaptively align semantic and structural signals across graphs.

**High-confidence Tuning** When target labels are unavailable, pseudo-labeling combined with data augmentation is a widely adopted strategy for mitigating distribution shift in unsupervised domain adaptation [3]. In the unlabeled target graph, we first generate pseudo-labels  $\hat{\mathcal{S}}_t$  using the well-calibrated pre-trained attack model and only preserve those nodes whose confidence scores exceed a pre-defined threshold  $\gamma$ . However, when the number of retained nodes is small or the target graph is limited in size, this few-shot scenario may lead to overfitting on noisy pseudo-labels. To alleviate data scarcity, we jointly fine-tune the attack model using both the auxiliary graph and the retained pseudo-labeled nodes. This strategy further aligns with auxiliary attack semantics while avoiding catastrophic forgetting, thereby enabling stable and robust adaptation. Formally, this high-confidence tuning objective can be formulated as follows:

$$\mathcal{L}_{cnf} = \mathcal{L}_{att} + \sum_{i=1}^s \sum_{j=1}^m w_i \cdot l(\hat{\mathcal{S}}_{tij}, \hat{\mathcal{S}}_{tij}) \mathbb{I}(\max P(\hat{\mathcal{S}}_{tij}) \geq \gamma) \quad (4)$$

where  $m \leq |\mathcal{V}_t|$  is the number of target nodes in the target graph,  $\mathbb{I}(\cdot)$  represents the indicator function,  $P(\cdot)$  denotes the predicted probability and  $\gamma$  is the pre-defined threshold.

**Adaptive Prototype Adjustment** A remaining challenge lies in the filtered nodes. As the pre-trained attack model cannot provide reliable confidence estimates for these nodes, semantic misalignment may persist between the auxiliary and target graphs. Thus, we introduce the *Adaptive Prototype Adjustment* submodule to align prototypes across graphs.

We first initialize class prototypes for each attack task using node embeddings from the auxiliary graph, which serve as reliable semantic anchors. Formally, the prototype  $\mathbf{C}$  for class  $k$  of attack task  $\mathcal{S}_i$  at iteration  $t$  is defined as:

$$\mathbf{C}_{\mathcal{S}_i, k}^t = \frac{\sum_{j=1}^{m+|\mathcal{V}_a|} \mathbb{I}(\mathcal{S}_i = k) Z_{\mathcal{S}_i}}{\sum_{j=1}^{m+|\mathcal{V}_a|} \mathbb{I}(\mathcal{S}_i = k)} \quad (5)$$

We further incorporate exponential moving average (EMA) [23] to enable smooth domain adaptation.

$$\mathbf{C}_{\mathcal{S}_i, k}^{t*} = \alpha \mathbf{C}_{\mathcal{S}_i, k}^{t-1} + (1 - \alpha) \mathbf{C}_{\mathcal{S}_i, k}^t \quad (6)$$

where the momentum  $\alpha \in [0, 1]$  controls the update rate.

For the filtered nodes, we define the following loss:

$$\mathcal{L}_{fil} = - \sum_{i=1}^s \sum_{j=1}^{m_{fil}} P(\hat{\mathcal{S}}_{ij}) \log\{P(\hat{\mathcal{S}}_{ij})\} \quad (7)$$

where  $m_{fil}$  denotes the number of filtered target nodes,  $P(\hat{\mathcal{S}}_{ij}) = \text{softmax}(\cos(Z_{fil, \mathcal{S}_i, j}, \mathbf{C}_{\mathcal{S}_i}) / \tau)$  is the prediction for each attack task and  $\tau$  is the temperature coefficient.

To align two graphs' distributions while mitigating catastrophic forgetting, we define the overall adaptation loss as:

$$\mathcal{L}_{prm} = \mathcal{L}_{cnf} + \mathcal{L}_{fil} \quad (8)$$

Notably, when auxiliary and target graphs originate from different distributions with mismatched feature dimensionalities (i.e., heterogeneous UDA), we apply principal component analysis (PCA) to project both graphs into a unified feature space. Our goal is to demonstrate the feasibility of G-MSAIAs under diverse auxiliary data settings, more advanced heterogeneous UDA techniques are left for future work.

### 3.3 Evaluation Metrics

Existing evaluation metrics for AIAs are primarily designed for a single sensitive attribute and therefore fail to capture the complexity of multi-attribute privacy leakage. To bridge this gap and answer our third research question, we propose a systematic evaluation framework for G-MSAIAs. We further empirically demonstrate its necessity in the following section. For clarity, we provide mathematical definitions for all metrics that are specific to the multi-attribute attack setting.

#### 3.3.1 Confidence-based Metrics

**Average AUC (AA) and F1 (AF).** We compute the standard AUC and F1 scores for each sensitive attribute and report their averages to provide a global assessment of attack confidence and discriminative capability in a unified way.

**Task Deviation AUC (TDA) and F1 (TDF).** To quantify the performance gap across attack tasks, for sensitive attribute  $\mathcal{S}_i$ , we define TDA as  $\max_{\mathcal{S}_i} \text{AUC}_{\mathcal{S}_i} - \min_{\mathcal{S}_i} \text{AUC}_{\mathcal{S}_i}$ , and TDF is defined analogously. Larger TDA/TDF indicates greater disparity and less stability across different attack tasks.

#### 3.3.2 Correctness-based Metrics

**Hamming Distance (HD)** HD quantifies the average fraction of incorrectly inferred sensitive attributes across all nodes. Mathematically, let  $\mathcal{S}_v$  and  $\hat{\mathcal{S}}_v \in \{0, 1\}^s$ , HD is defined as  $\text{HD} = \frac{1}{|\mathcal{V}|} \sum_{v \in \mathcal{V}} \frac{1}{s} \sum_{i=1}^s \mathbb{I}(\hat{\mathcal{S}}_{v,i} \neq \mathcal{S}_{v,i})$ .

**Subset Accuracy (SuA)** While HD captures marginal privacy leakage, it overlooks joint attack success across multiple sensitive attributes. To address this limitation, we introduce SuA, a strict “all-or-nothing” metric that measures the

probability of simultaneous G-MSAIAs, defined as  $\text{SuA} = \frac{1}{|\mathcal{V}|} \sum_{v \in \mathcal{V}} \frac{1}{s} \mathbb{I}(\hat{\mathcal{S}}_{v,1} = \mathcal{S}_{v,1}, \dots, \hat{\mathcal{S}}_{v,s} = \mathcal{S}_{v,s})$ . An attack is counted as successful under SuA only if all sensitive attributes of a specific node are correctly inferred. However, SuA alone can be misleading: a low SuA does not necessarily imply effective privacy protection, as partial leakage across attributes may still be substantial. In this sense, HD and SuA are complementary, HD reflects marginal leakage, while SuA captures joint compromise. Their combination provides a more comprehensive assessment of sensitive information erosion.

### 3.3.3 Semantics-based Metrics

Multiple sensitive attributes often exhibit complex internal correlations, however, existing metrics largely ignore this facet and therefore cannot assess whether an attack captures the underlying semantic dependencies of the target graph.

**Semantic Difference (SD)** SD measures the discrepancy in feature-label alignment between inferred and ground-truth sensitive attributes, defined as  $dCor(\hat{S}, X) - dCor(S, X)$ . Lower SD values indicate that the attack preserves more feature-to-label alignment, whereas higher SD suggests that the attack may overly rely on biased feature signals.

**Label Consistency (LC)** LC evaluates whether inferred sensitive attributes retain the dependency structure of the ground-truth, denoted as  $dCor(\hat{S}, S)$ . Higher LC indicates that the attack effectively captures internal correlations among multiple sensitive attributes while Lower LC suggests weak or distorted dependency modeling.

## 4 Experiments

In this section, we conduct extensive experiments on four real-world graph datasets to systematically evaluate the attack performance of Taipan. Specifically, we investigate the following six experimental questions:

**Q1:** Why is the comprehensive evaluation framework necessary for G-MSAIAs?

**Q2:** How effective is Taipan in performing G-MSAIAs?

**Q3:** How well does Taipan generalize across GNN encoders?

**Q4:** What factors can influence the performance of Taipan?

**Q5:** Which nodes are most vulnerable to Taipan?

**Q6:** How robust is Taipan against defense mechanisms?

### 4.1 Experiment Setups

**Datasets.** We evaluate Taipan on four real-world benchmark graph datasets: German, Credit, Pokec-n and Pokec-z. Graph statistics are presented in Table 6 in Appendix A.1.

**GNN encoders.** We consider three representative GNNs: GCN [19], GraphSAGE [15] and GIN [34]. Their original performance is summarized in Table 7 in Appendix A.4.

**Baselines.** Taipan is the first attack framework for G-MSAIAs. Existing AIA studies against GNNs either rely on access to

node embeddings or repeated queries to victim GNNs [12, 25], and are not directly comparable. Therefore, we consider the following baselines: (1) Random Guessing (Rand.): Sensitive attributes are inferred by random sampling from Bernoulli distributions based on empirical class priors. This baseline is only used for comparison. (2) Single Prediction (SingP.): We separately train an attack model for each sensitive attribute, and then aggregate the best-performing models. SingP. also serves as an ablation without attack hierarchy and the “attack transfer” paradigm. (3) Pre-training (PreTr.): We directly apply pre-trained Taipan to infer multiple sensitive attributes on the target graph. This baseline also acts as an ablation without *Prompt-guided Attack Prototype Refinement*.

**Implementation.** Experiments are conducted on three Nvidia A100 GPUs. Please see Appendix A.3 for more details.

## 4.2 Attack Performance (Q1-Q3)

### 4.2.1 Necessity of Comprehensive Evaluation (Q1)

The attack results in Table 2 highlight the limitations of classical single-attribute metrics. Under class imbalance, even random guessing can yield deceptively high average AUC and F1 scores, but their task deviations are substantial, e.g., Rand. on German, which indicates that poor performance on certain attack tasks can be obscured by strong performance on others. Correctness-based metrics further reveal these shortcomings. For instance, while Rand. attains acceptable HD, its SuA drops sharply, suggesting weak joint inference across multiple sensitive attributes. Similarly, SingP. exhibits low SuA, as independently trained attack models may behave inconsistently on the same node samples, leading to severe performance degradation in the multi-attribute setting. In contrast, SuA can better capture inference synergy across multiple sensitive attributes. The competitive SuA achieved by pre-trained and full Taipan supports this observation, as Taipan is designed to model task correlations and mitigate negative transfer. Notably, low SuA alone does not imply strong privacy protection when HD still indicates substantial partial leakage, such as SingP. on German. Finally, the semantics-based metrics assess whether inferred attributes align with sensitive attributes in the auxiliary graphs. Consistent with earlier findings, SD reveals that GCN tends to induce higher bias, while LC shows that Taipan can effectively capture intersectional correlations among multiple sensitive attributes.

### 4.2.2 Effectiveness (Q2)

From Table 2, we observe consistent patterns of Taipan across diverse graph datasets. Both Taipan and its pre-trained variant (PreTr.) outperform random guessing and achieve performance comparable to or exceeding SingP. across most evaluation metrics. Specifically, full Taipan generally maintains superior performance over PreTr., highlighting the effectiveness of *Prompt-guided Attack Prototype Refinement*. We note

that while SingP. attains higher AA and AF in some cases, it yields unstable and unfair attack performance, as reflected by TDA and TDF, and significantly lags behind Taipan in correctness and semantics-based metrics. For instance, on Pokec-n with GraphSAGE as the encoder, SingP. exceeds Taipan by 4.57% in AA, yet performs worse in AF and incurs substantially larger task deviations. Overall, Taipan not only achieves comparable or higher AA/AF than SingP. but also demonstrates superior stability and fairness while more effectively preserving intersectional sensitive correlations. We further visualize node embeddings of the inferred multiple sensitive attributes along with their joint confidence score distributions to illustrate the effectiveness of Taipan. Due to space limitations, details are provided in Appendix A.5.

### 4.2.3 Flexibility (Q3)

As shown in Table 2, Taipan and PreTr. exhibit robust performance across all GNN encoders. In general, attack performance degrades with GIN as the encoder. The only exception occurs on the dense Credit graph. Unlike GCN and GraphSAGE, which employ smoothing “low-pass” filters, GIN relies on sum-based aggregation and is therefore more sensitive to structural noise, particularly on graphs with low average degree. This behavior is consistent with the lower original performance of GIN on such graphs, suggesting a fundamental mismatch between its aggregation mechanism and the underlying graph structure. Furthermore, the additional learnable parameters introduced by pretext tokens may amplify noise, impairing transferable knowledge extraction and semantic alignment, as reflected by SD and LC.

### 4.2.4 Ablation Studies (Q4)

To systematically assess the contribution of each component in Taipan, we conduct a series of ablation studies on German with GCN as the encoder. In *Hierarchical Attack Knowledge Routing*, we separately remove the attack hierarchy, pretext tokens, and the gating mechanism, along with their combinations. In *Prompt-guided Attack Prototype Refinement*, we ablate the source-based prototype adjustment. As target-based adaptation constitutes the core design of this module, removing it entirely reduces the framework to the pre-trained Taipan. As shown in Table 3, removing any component results in a clear degradation in attack performance, with the extent of degradation reflecting its relative importance. Particularly, pretext tokens contribute the most to G-MSAIAs, followed by the attack hierarchy. The combination of pretext tokens and the gating mechanism yields the strongest gains for partial sensitive attribute inference while the combination of pretext tokens and the attack hierarchy follows behind. Source-based prototype adjustment further provides a performance gain in *Prompt-guided Attack Prototype Refinement*. Overall, *Hierarchical Attack Knowledge Routing* plays a central role in

Table 2: The Attack Performance of Taipan for G-MSAIAs — Same-distribution Transfer. **Bold**: Best result; **Underline**: Second best result (close to the best).

Dataset	GNN	Baseline	AA (↑)	AF (↑)	TDA (↓)	TDF (↓)	HD (↓)	SuA (↑)	SD (↓↓)	LC (↑)
	Real Value	Rand.	54.21	60.25	13.08	58.70	36.33	26.00	-2.28	20.37
German	SingP.	<b>66.50</b>	42.50	13.46	88.05	33.27	14.00	<b>0.48</b>	34.36	
	GCN	66.34	73.62	<b>10.45</b>	40.24	<b>20.33</b>	<b>54.00</b>	<b>7.22</b>	42.77	
	PreTr.	<b>70.01</b>	<b>76.10</b>	<b>7.58</b>	<b>31.44</b>	<b>21.33</b>	<b>57.00</b>	9.88	<b>46.35</b>	
	Taipan	<b>70.01</b>	<b>76.10</b>	<b>7.58</b>	<b>31.44</b>	<b>21.33</b>	<b>57.00</b>	9.88	<b>46.35</b>	
	GraphSAGE	69.47	54.72	<b>8.28</b>	55.69	35.20	35.20	<b>-1.80</b>	32.43	
	Taipan	<b>69.37</b>	<b>70.49</b>	19.95	53.75	19.67	53.00	6.26	56.15	
Credit	SingP.	72.62	<b>77.11</b>	16.99	<b>41.41</b>	<b>16.33</b>	<b>60.00</b>	<b>3.38</b>	<b>64.40</b>	
	GCN	55.64	31.49	22.18	89.50	34.80	12.00	<b>-8.37</b>	6.89	
	PreTr.	<b>66.39</b>	<b>73.38</b>	<b>21.16</b>	<b>33.26</b>	<b>25.00</b>	<b>49.00</b>	<b>9.39</b>	57.20	
	Taipan	<b>67.30</b>	<b>72.28</b>	<b>5.70</b>	<b>28.12</b>	<b>30.67</b>	39.00	18.91	<b>62.58</b>	
	Real Value	Rand.	49.97	72.31	0.30	36.30	33.47	41.63	-5.50	1.37
	GraphSAGE	<b>62.80</b>	<b>82.63</b>	21.14	<b>24.48</b>	27.60	46.16	<b>4.70</b>	9.12	
Pokec-n	GCN	57.18	<b>80.94</b>	5.13	28.16	<b>24.30</b>	<b>53.67</b>	<b>5.03</b>	<b>19.34</b>	
	PreTr.	<b>60.02</b>	<b>76.16</b>	<b>6.95</b>	<b>25.53</b>	<b>26.13</b>	<b>51.37</b>	19.38	15.91	
	Taipan	<b>69.69</b>	<b>78.99</b>	<b>4.87</b>	<b>31.66</b>	<b>24.97</b>	<b>53.77</b>	<b>9.17</b>	<b>19.62</b>	
	GraphSAGE	60.45	77.96	<b>5.54</b>	34.77	<b>25.40</b>	<b>52.40</b>	<b>9.08</b>	16.24	
	PreTr.	61.86	<b>78.91</b>	<b>4.87</b>	<b>31.66</b>	<b>24.97</b>	<b>53.77</b>	<b>9.17</b>	<b>19.62</b>	
	Taipan	<b>66.69</b>	<b>81.30</b>	<b>8.58</b>	<b>28.00</b>	<b>22.78</b>	<b>56.90</b>	<b>1.52</b>	<b>26.24</b>	
Pokec-z	Real Value	Rand.	48.40	28.30	4.60	23.50	41.67	21.70	-6.41	8.01
	SingP.	<b>81.06</b>	57.14	21.14	32.62	22.18	46.22	<b>-0.04</b>	44.37	
	GCN	72.34	61.01	15.13	27.91	<b>20.76</b>	<b>50.11</b>	<b>2.82</b>	<b>48.23</b>	
	PreTr.	<b>74.85</b>	<b>64.39</b>	<b>10.80</b>	<b>20.46</b>	<b>21.74</b>	46.93	4.85	<b>47.76</b>	
	Taipan	<b>81.76</b>	63.39	29.84	40.75	20.82	48.69	4.55	56.71	
	GraphSAGE	77.12	<b>66.68</b>	<b>21.06</b>	<b>32.15</b>	<b>18.45</b>	<b>54.20</b>	<b>3.23</b>	<b>59.74</b>	
Taipan	GIN	<b>77.48</b>	55.25	19.64	31.62	24.01	42.31	<b>-0.17</b>	41.21	
	PreTr.	69.74	<b>57.88</b>	10.17	<b>21.11</b>	<b>21.89</b>	<b>47.05</b>	<b>0.23</b>	<b>44.24</b>	
	Taipan	<b>70.89</b>	<b>58.96</b>	<b>11.52</b>	<b>25.25</b>	<b>21.67</b>	<b>47.27</b>	1.45	<b>44.89</b>	
	Real Value	Rand.	50.28	37.07	4.50	25.89	42.94	18.40	-9.31	6.45
	SingP.	<b>80.18</b>	59.15	<b>22.85</b>	<b>34.17</b>	23.53	44.55	<b>0.49</b>	43.43	
	GCN	76.53	67.78	28.28	41.21	<b>18.70</b>	<b>53.16</b>	<b>2.44</b>	<b>61.83</b>	
Taipan	PreTr.	<b>80.28</b>	<b>73.14</b>	<b>25.51</b>	<b>31.96</b>	<b>19.51</b>	<b>52.87</b>	4.53	<b>61.05</b>	
	GraphSAGE	78.69	<b>70.68</b>	<b>21.90</b>	<b>31.46</b>	<b>18.44</b>	<b>54.92</b>	5.95	<b>60.81</b>	
	PreTr.	<b>80.49</b>	<b>72.70</b>	<b>20.19</b>	<b>29.15</b>	<b>17.66</b>	<b>56.28</b>	<b>5.86</b>	<b>61.90</b>	
	Taipan	<b>78.06</b>	59.96	20.76	28.16	25.38	40.91	<b>0.06</b>	41.35	
	GIN	74.28	<b>67.39</b>	9.43	<b>17.41</b>	<b>22.65</b>	46.25	<b>-1.11</b>	47.49	
	Real Value	Taipan	<b>76.96</b>	<b>69.87</b>	11.99	16.57	20.64	<b>50.05</b>	3.77	<b>51.92</b>

Taipan for effective G-MSAIAs.

Table 3: The Ablation Studies of Taipan for G-MSAIAs

Stage	Variant	AA (↑)	AF (↑)	TDA (↓)	TDF (↓)	HD (↓)	SuA (↑)	SD (↓↓)	LC (↑)
Full	Taipan	<b>70.01</b>	<b>76.10</b>	<b>7.58</b>	<b>31.44</b>	21.33	<b>57.00</b>	9.88	<b>46.35</b>
Pre-training	w.o.hierarchy	64.65	67.35	21.29	54.77	25.33	49.00	5.02	44.99
	w.o.pretexts	58.06	71.53	12.84	46.41	25.00	54.00	3.73	39.42
	w.o.gating	<b>67.32</b>	70.50	21.71	<b>35.34</b>	28.33	44.00	15.64	<b>51.77</b>
	w.o. hier.+pre.	54.72	67.57	11.71	54.35	25.33	55.00	<b>3.19</b>	37.91
	w.o. hier.+gate	63.40	68.38	<b>7.53</b>	52.20	24.67	<b>56.00</b>	<b>3.29</b>	38.08
	w.o. all	58.91	66.39	18.83	61.89	22.67	52.00	15.93	36.90
Prompt-tuning	w.o. source adjust.	<b>67.92</b>	<b>74.95</b>	14.23	<b>35.59</b>	<b>20.67</b>	54.00	11.42	<b>46.58</b>
	w.o.all	66.34	73.62	10.45	40.24	<b>20.33</b>	54.00	7.22	42.77

### 4.3 Impact Factors (Q4 and Q5)

#### 4.3.1 Heterogeneous Attack Transfer (Q4)

Previously, we assumed the auxiliary graph is drawn from the same distribution as the target graph. We now consider a more challenging setting where adversaries can only access heterogeneous auxiliary graphs, including both similar-distribution and OOD cases. Specifically, we study two transfer scenarios: (1) Pokec-n as the auxiliary graph and Pokec-z as the target graph, which originate from the same social network but are sampled from different provinces and exhibit mismatched feature dimensionalities; and (2) Credit as the auxiliary graph and German as the target graph, which stem from different data sources with distinct learning objectives. From Table 4, Taipan and PreTr. consistently outperform SingP. across diverse GNN encoders and transfer configurations. Consistent with earlier observations, GIN yields inferior attack perfor-

mance in the Pokec-n-to-Pokec-z transfer. While the Credit-to-German transfer introduces larger distribution shifts and results in lower attack performance than Pokec-n-to-Pokec-z, Taipan remains effective under this stringent setting.

Table 4: The Attack Performance for G-MSAIAs —  
Heterogeneous Similar-distribution and  
Out-of-distribution Transfers

Dataset	GNN	Baseline	AA (↑)	AF (↑)	TDA (↓)	TDF (↓)	HD (↓)	SuA (↑)	SD (↓↓)	LC (↑)
Pokec-n—Pokec-z	GCN	SingP.	<b>71.37</b>	43.15	35.58	<b>49.14</b>	<b>29.10</b>	<b>34.92</b>	<b>-2.01</b>	33.67
		PreTr.	62.22	44.87	<b>24.50</b>	51.88	<b>29.18</b>	<b>34.08</b>	-3.75	<b>37.51</b>
		Taipan	64.33	<b>50.61</b>	<b>23.66</b>	<b>41.87</b>	29.83	32.04	<b>2.77</b>	<b>36.14</b>
	GraphSAGE	SingP.	<b>73.01</b>	50.77	36.87	48.06	<b>27.27</b>	<b>37.36</b>	<b>-0.77</b>	43.40
		PreTr.	64.64	<b>52.16</b>	29.43	<b>42.74</b>	29.21	33.89	-1.80	<b>40.62</b>
		Taipan	65.79	<b>55.29</b>	<b>25.77</b>	<b>36.34</b>	<b>28.89</b>	<b>34.86</b>	<b>0.53</b>	40.35
	GIN	SingP.	<b>66.62</b>	47.33	23.48	30.56	32.10	30.07	<b>-0.16</b>	26.92
		PreTr.	58.02	36.21	17.04	54.77	<b>30.28</b>	33.79	<b>-4.41</b>	<b>29.96</b>
		Taipan	<b>64.22</b>	<b>54.71</b>	13.32	<b>23.70</b>	<b>30.67</b>	<b>32.72</b>	7.78	<b>30.93</b>
Credit—German	GCN	SingP.	44.25	69.11	17.56	40.30	39.10	33.00	43.49	19.82
		PreTr.	47.20	<b>75.34</b>	<b>5.60</b>	<b>31.93</b>	<b>34.00</b>	40.00	45.62	23.15
		Taipan	<b>50.75</b>	<b>74.22</b>	<b>1.51</b>	<b>34.16</b>	<b>32.00</b>	<b>44.00</b>	<b>31.37</b>	5.88
	GraphSAGE	SingP.	<b>50.74</b>	<b>71.06</b>	3.28	34.37	<b>35.50</b>	<b>38.60</b>	<b>-8.62</b>	5.90
		PreTr.	48.74	<b>68.29</b>	<b>1.03</b>	<b>26.84</b>	<b>40.50</b>	<b>37.00</b>	<b>11.96</b>	<b>29.35</b>
		Taipan	<b>51.93</b>	66.30	<b>2.96</b>	<b>3.57</b>	44.50	33.00	35.42	<b>29.36</b>
	GIN	SingP.	<b>51.66</b>	<b>78.44</b>	4.69	<b>15.27</b>	<b>34.70</b>	<b>46.00</b>	<b>-10.37</b>	4.08
		PreTr.	46.91	68.17	0.23	40.19	<b>37.50</b>	38.00	<b>10.84</b>	9.27
		Taipan	<b>54.28</b>	<b>70.91</b>	<b>1.25</b>	<b>9.46</b>	42.00	34.00	43.01	<b>13.97</b>

### 4.3.2 Adaptation Steps (Q4)

We assess the impact of adaptation steps in Taipan for G-MSAIAs and present the main results in Figure 3. Additional details on semantic-based metrics are provided in Figure 9 in Appendix A.6. We observe a consistent trend across graphs: confidence and semantic-based metrics improve rapidly within a small number of adaptation steps, followed by oscillation or mild degradation as adaptation continues. This trend indicates that most transferable attack semantic signals are captured during early adaptation, while additional steps provide limited marginal benefits or induce instability. Meanwhile, correctness-based metrics exhibit only slight degradation within small adaptation steps, as reflected by the narrow y-axis range. From a practical standpoint, these observations suggest that a small number of adaptation steps is sufficient to achieve strong attack performance, offering a favorable trade-off between effectiveness and computational overhead. We further observe that the relative performance of different graphs varies substantially across all metrics. Such variations stem from a combination of intrinsic graph characteristics (e.g., node degree distribution, homophily, and data imbalance) and task-level factors, including inter-attribute correlations and learning difficulty. For instance, although Credit exhibits relatively weaker confidence-based performance, it attains comparable SuA due to its limited number of sensitive attributes and simple task correlations.

### 4.3.3 Node Degree and Node Homophily (Q4 and Q5)

Building upon our prior analysis of impact factors across node, group, task-levels, we investigate the two node-level factors, namely node degree and homophily, to identify the most vulnerable nodes and simultaneously examine their corresponding impacts on attack performance. We visualize the

relationship between node degree, node homophily, and per-node subset accuracy in Figure 4. Notably, these scattered points exhibit degree-dependent patterns but not linear trends. Since we evaluate subset accuracy at the node level, this “all-or-nothing” metric is inherently discrete, yielding values of either 0 or 1 for individual nodes. For brevity, we defer the details of per-node attack accuracy defined over range [0, 1] in Figure 10 in Appendix A.7. We observe that node degree exhibits a strong positive correlation with subset accuracy, particularly on German and Pokec-z. Intuitively, nodes with higher degree aggregate information from larger neighborhoods, thereby providing richer and more stable structural signals for G-MSAIAs. We also observe a clear positive relationship between node homophily and attack success across all graphs. When neighboring nodes tend to share the same sensitive attributes, the message-passing mechanism reinforces consistent semantic and structural signals, reducing noise and amplifying confidence in attribute inference. In conclusion, these observations indicate that nodes embedded in dense and homophilic regions are more vulnerable to G-MSAIAs.

## 4.4 Defense (Q6)

In this section, we utilize two defense mechanisms to assess their effectiveness against Taipan. These defenses also serve as representative case studies for evaluating Taipan under privacy-preserving graph publishing techniques.

### 4.4.1 Differential Privacy

We first adopt the standard privacy-preserving mechanism—differential privacy (DP)—to provide rigorous privacy guarantees. Even though DP is primarily designed to protect individual membership information by injecting noise into either the data or the training process, it has also been widely employed to defend against AIAs [17, 44]. Since Taipan operates in a query-free data-only setting, DP-protected GNN training is not applicable. Instead, we resort to DP graph synthesis. However, existing DP graph synthesis methods mainly focus on edge-level DP, which protects the presence or absence of individual edges [35, 38]. Enforcing node-level DP is substantially more challenging, as modifying a single node induces high sensitivity due to the removal of all incident edges, particularly for high-degree nodes.

To assess the impact of DP on Taipan, we leverage the state-of-the-art DP graph synthesis method, PrivDPR [42], which achieves  $(\epsilon, \delta)$ -node DP via deep PageRank. Following the default configuration of PrivDPR, we fix the privacy budget  $\epsilon$  to 0.1 and evaluate Taipan under a stringent  $(0.1, 1e-5)$  node-DP guarantee. Our objective is not to preserve a favorable privacy–utility trade-off, but rather to stress-test Taipan under rigorous privacy protection.

As shown in Table 5, node-DP fails to effectively defend against Taipan. In dense and highly homophilic graphs like

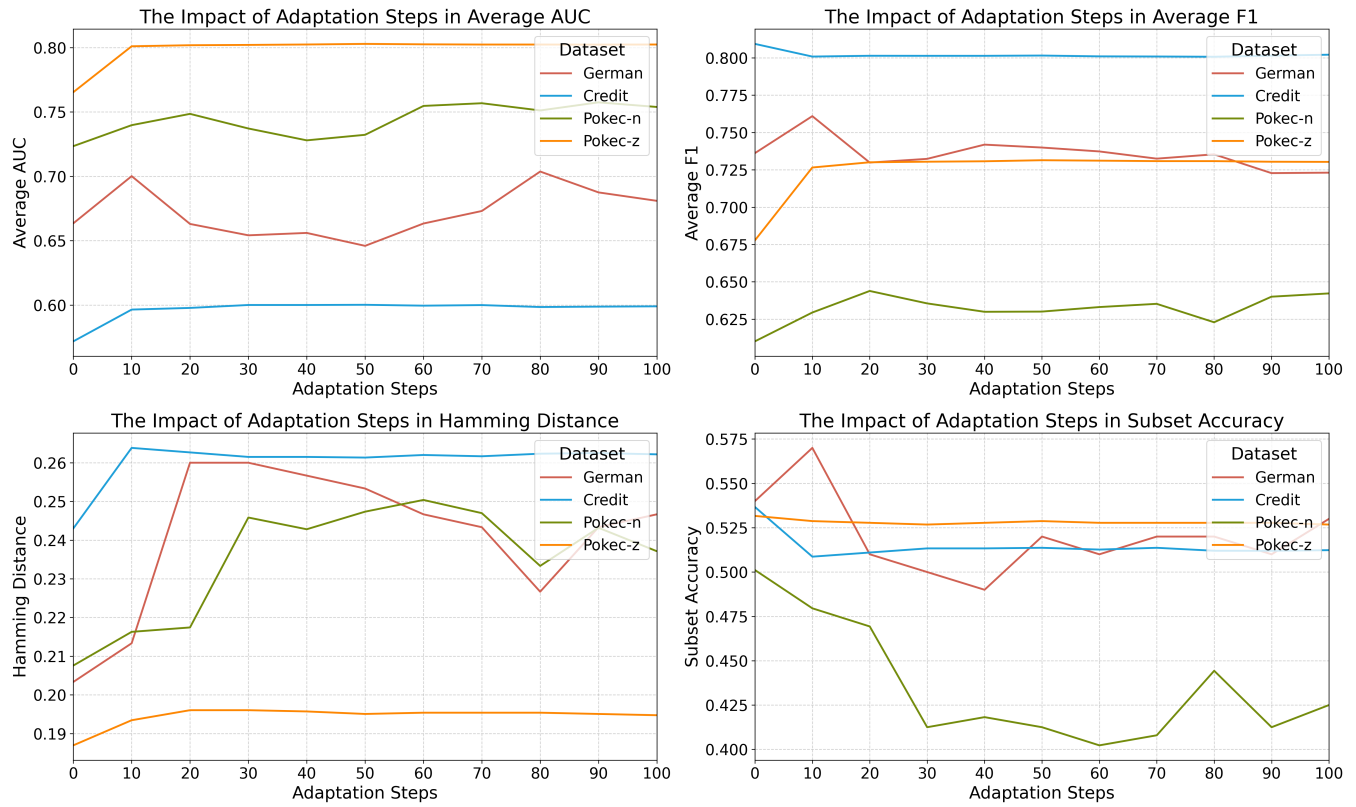


Figure 3: Impact of Adaptation Steps

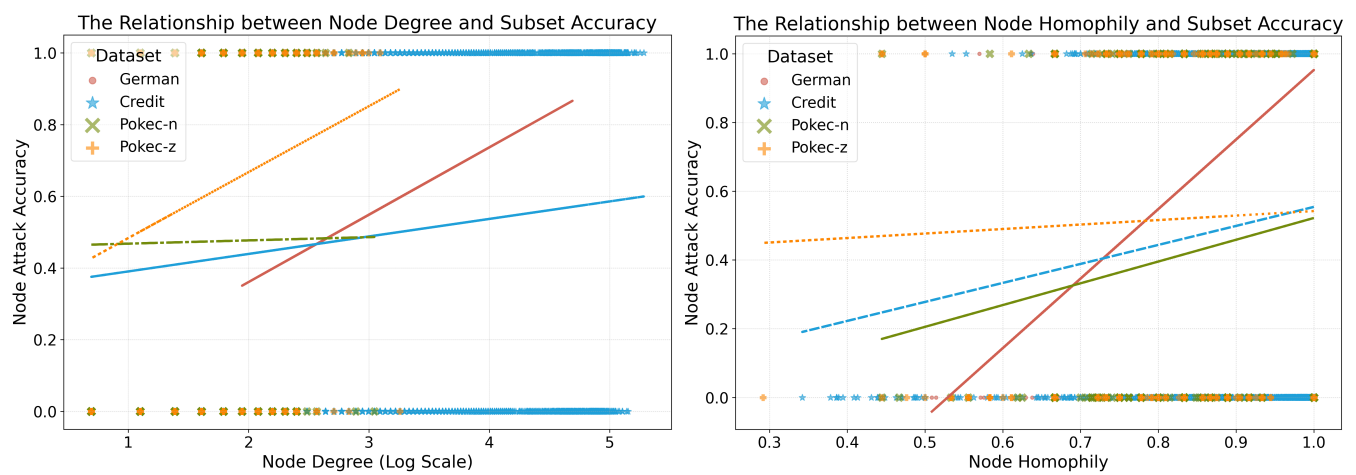


Figure 4: Impacts of Node Degree and Node Homophily

Credit, the attack performance under a strict node-DP guarantee closely resembles that of Taipan without any defense. On German, attack performance remains strong across nearly all metrics. While AA is comparable on Pokec-n and Pokec-z, AF substantially degrades and becomes unstable and unfair across different attack tasks. We speculate that this large performance drop stems from the poor synthetic quality, as the downstream GNN performances on the synthesized Pokec-n and Pokec-z are only 64.07%, 52.84%, 43.65%, and 65.80%, 47.61%, 39.85% in AUC, ACC and F1, respectively. Since traditional utility-based metrics are model-dependent and typically tailored to a single attribute attribute, they are insufficient to capture multi-attribute privacy leakage on graphs. Motivated by these limitations, we resort to a 2-layer GCN without nonlinear activations to obtain node embeddings while mitigating nonlinear noise. We then leverage *dCor* to measure sensitive correlations between node embeddings  $Z$  and multiple sensitive attributes and report *dCor* on the original ( $ODC = (Z_t, \mathcal{S})$ ) and on the synthetic target graphs ( $DDC = (\tilde{Z}_t, \mathcal{S})$ ) in Table 5. Our results show that although strict node-DP largely reduces sensitive correlations, the residual correlations can still be exploited by Taipan for multiple sensitive attribute inference.

Table 5: The Defense against Taipan for G-MSAIAs

Defense	Dataset	AA (↑)	AF (↑)	TDI (↓)	TDF (↓)	HD (↓)	SuA (↑)	SD (↓↑)	LC (↑)	ODC (↓)	DDC (↓)
Node-DP	German	58.16	63.87	4.92	55.04	29.67	41.00	12.28	21.96	24.00	8.61
	Credit	51.08	70.53	0.18	45.29	31.20	44.77	33.51	3.59	6.43	2.63
	pokec-n	65.91	51.96	13.33	35.21	26.14	40.91	-5.06	36.73	11.56	5.77
	pokec-z	73.34	65.44	33.76	40.87	22.62	45.37	0.86	56.30	33.09	17.21
FairGNN	German	64.94	70.96	9.88	46.31	26.67	49.00	8.71	37.15	24.00	10.13
	Credit	54.16	79.78	4.26	29.83	27.92	46.93	21.48	6.79	6.43	5.94
	pokec-n	71.43	55.80	22.20	46.78	21.93	48.18	5.40	49.81	11.56	11.13
	pokec-z	79.53	72.74	27.50	33.08	20.55	50.83	4.56	60.01	33.09	14.51

#### 4.4.2 Fair Learning

Following Dibbo et al. [11], we leverage fair graph learning to mitigate AIAs. To the best of our knowledge, MAPPING [27] is the only existing method that explicitly handles multiple sensitive attributes prior to GNN training. It demonstrates that fairness interventions can effectively remove sensitive correlations between multiple sensitive attributes and model predictions, thereby reducing sensitive information leakage. Accordingly, we employ MAPPING to generate debiased synthetic graphs with reduced privacy leakage.

We follow the default configuration of MAPPING and fix its fairness-relevant coefficients to  $\lambda_2 = 3.5e-5$ ,  $\lambda_3 = 50$ ,  $\lambda_2 = 1e-4$  and  $r_p = 0.72$  across all graphs. Compared to strict node-DP, attack performance on MAPPING-generated graphs is consistently higher for both average single-attribute inference and joint multi-attribute inference. In particular, on Pokec-n and Pokec-z, downstream GNN performance improves to 71.25%, 57.61%, 51.10% and 75.32%, 55.21%, 49.53% in terms of AUC, ACC and F1, respectively, indicating substantially better synthetic quality. Correspondingly, sensitive correlations also increase. The only exception occurs for DDC on Pokec-z, where the sensitive correlation

under node-DP is slightly higher than that under MAPPING. A plausible explanation is that PrivDPR primarily enforces node-level privacy by aggressively pruning edges, which may overly suppress informative structural signals required for multiple sensitive attribute inference. Moreover, PrivDPR does not explicitly remove sensitive traces from node features, resulting in relatively larger DDC. In contrast, MAPPING jointly mitigates sensitive signals in both node features and graph topology, achieving a better trade-off between fairness and utility. The enhanced synthesis quality further translates into stronger attack performance.

## 4.5 Limitations and Future Work

**Extreme Domain Shifts** With the rapid progress of transfer learning under extreme domain shifts, an important future direction is to extend Taipan to scenarios where auxiliary graphs from the same or similar domains are unavailable or impractical to obtain.

**Very Large-scale Graph Dataset** Although Taipan has been evaluated on large-scale graphs, extending it to very large-scale graph datasets remains an open challenge. Addressing scalability in such settings would further enhance its practical applicability and real-world impact.

**Deep Investigation on Vulnerable Nodes** While we identify several key impact factors that influence G-MSAIAs, a more in-depth investigation should be conducted to analyze the intricate interplays among these factors and to uncover potential synergistic or conflicting effects across multiple attack tasks.

**Multi-class and Multi-task Types** Taipan can be naturally generalized to multi-class settings and regression-based attack tasks. These extensions still necessitate a deeper investigation of the complex interactions among multiple sensitive subgroups and individuals.

## 5 Conclusion

In this work, we pioneer the investigation of an inherent yet unexplored vulnerability arising solely from publicly released graphs. We introduce a new attack paradigm for G-MSAIAs through “multi-task attack transfer”, and propose Taipan, the first query-free transfer-based attack framework that extracts shared and task-specific attack knowledge from auxiliary graphs to simultaneously infer multiple sensitive attributes on target graphs. By integrating *Hierarchical Attack Knowledge Routing* with *Prompt-guided Attack Prototype Refinement*, Taipan effectively mitigates distribution shift between auxiliary and target graphs under realistic data-only settings. Extensive experiments on real-world graph datasets demonstrate that Taipan achieves strong attack performance even under rigorous privacy safeguards. Our findings highlight an urgent need to re-examine the privacy risks posed by publicly released graphs and establish more robust multi-attribute privacy-preserving graph publishing practices.

## APPENDIX

### Ethical Considerations

This research identifies a critical yet unexplored vulnerability that adversaries can solely exploit publicly released graphs to conduct multiple sensitive attribute inference attacks. We introduce a new query-free transfer-based attack paradigm and demonstrate its substantial privacy risks in same or similar-distribution and out-of-distribution settings. To mitigate privacy concerns and prevent potential data misuse, we only utilize publicly available datasets that have been extensively adopted in prior research. All experiments are conducted on local devices in controlled environments. No personally identifiable information is disclosed, and no real-world systems or servers are compromised.

Massive datasets are increasingly published for research or commercial purposes, or are easily acquired via web-scraping or data breaches. However, existing defense mechanisms are predominantly model-centric and designed to protect against single sensitive attribute leakage, and therefore cannot effectively defend against the proposed attacks. It is imperative for researchers to develop more robust and reliable multiple-attribute privacy-preserving graph publishing methods, and for practitioners to re-evaluate current data-sharing practices. Furthermore, we call upon policymakers to strengthen corresponding data protection regulations.

The techniques, models, and open-sourced codes provided in this paper are intended only for research purposes or for improving data privacy protection in real-world applications.

### Open Science

In compliance with the CFP Open Science policy, we publicly release our datasets, source code, and evaluation scripts. To promote reproducibility and transparency, these materials are packaged in an anonymous repository <https://anonymous.4open.science/r/Taipan-2D34>. The formal GitHub repository will be released upon acceptance. These resources are intended to facilitate further research, enable rigorous assessment of multiple sensitive information leakage, and support the development of more effective and robust data privacy safeguards.

## A Experiments

### A.1 Data Statistics

German and Credit are financial credit networks constructed by Agarwal et al. [2]. In German, nodes represent bank clients and edges are constructed if two clients exhibit high similarity in their credit accounts. The task is to classify credit risk as high or low given three sensitive attributes—marriage status, gender, and age. In Credit, nodes denote credit card

users and edges are formed based on similarity in payment behaviors. The task is to predict whether an applicant will default on an upcoming payment considering two sensitive attributes—marriage status and age. Pokec-n and Pokec-z [31] are derived from a popular social network application in two different provinces of Slovakia, respectively. Nodes are application users and edges represent friendship relations. The task is to predict the working field of the users with three sensitive attributes—region, gender and age.

Table 6: **Detailed Graph Statistics.** Imb. Ratio: #majority/#minority, where 1 indicates perfect balance.

Dataset	#Nodes	#Edges	#Attr.	#SAs	Label	Avg. Deg.	Homo. (%)	Imb. Ratio Range
German	1,000	22,242	27	3	Credit Status	44.48	60.86	[1.15-3.68]
Credit	30,000	1,436,858	13	2	Payment Default	95.79	72.55	[1.20-10.17]
Pokec-n	66,569	583,616	266	3	Working Field	16.53	79.79	[1.05-2.65]
Pokec-z	67,796	617,958	277	3	Working Field	19.23	77.05	[1.02-2.77]

### A.2 Attack Task Correlation and Hierarchy

The attack task correlations and corresponding hierarchy of all graph datasets are illustrated in Figure 5 and 6.



Figure 5: The Attack Task Correlations among Diverse Graph Datasets

### A.3 Implementation Details

We adopt the architecture design of GCN, GraphSAGE and GIN in existing studies [2, 27], and follow standard practice [26, 40, 43] to split each graph dataset into two equal parts: one serving as the victim graph and the other as the auxiliary graph. The splitting ratio is 6/2/2 for training, validation and testing, respectively. To maintain consistent loss scales and ensure stable optimization, we adopt the averaged form for each loss function. We provide the hyperparameter settings for different stages as follows.

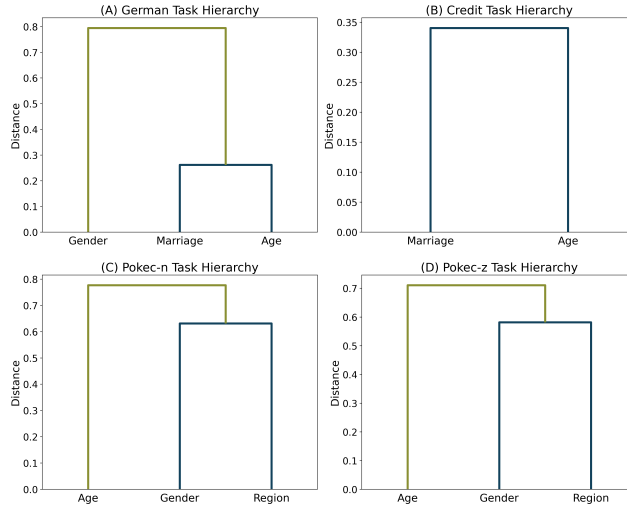


Figure 6: The Attack Hierarchy of Diverse Graph Datasets

1. **Victim GNN:** The hidden layer dimension is set to 16 for German and Credit and 64 for Pokec-n and Pokec-z. The learning rate is 0.01, weight decay is  $5e-4$  and dropout rate is 0.05. The number of training epochs is 1000 for German and Credit and 200 for Pokec-n and Pokec-z. We use Adam as the optimizer.
2. **Taipan:** During *Hierarchical Attack Knowledge Routing*, we adopt the same setting, except for learning rate  $\in \{0.005, 0.01\}$ . During *Prompt-guided Attack Prototype Refinement*, the adaptive threshold is tuned from  $\{0.5, 0.6, 0.7, 0.8\}$ , the number of adaptation steps is from  $\{10, 20, 30, 40, 50\}$ , and learning rate is from  $\{0.001, 0.005, 0.01\}$ . We follow the standard and set momentum as 0.9 and temperature as 0.1.
3. **Baselines:** For Rand., we utilize the empirical frequencies of sensitive attributes for Bernoulli sampling. For SingP., learning rate is tuned from  $\{0.001, 0.005\}$  while other settings remain identical.

#### A.4 Original Performance

From Table 7, we observe that GraphSAGE consistently outperforms GCN and GIN; GCN exceeds GIN on small-scale datasets, while GIN excels on large-scale datasets. Since attribute privacy is closely aligned with group fairness [1, 27], as both aim to limit the model’s reliance on sensitive attributes, we adopt two widely used group fairness metrics to provide indirect evidence of sensitive information leakage: statistical parity difference ( $\Delta SP$ ) and equalized odds difference ( $\Delta EO$ ), which measure prediction rate disparity and discrepancies in true/false positive rates across sensitive groups, respectively [1, 32]. However, our results indicate that these conventional metrics fail to reliably capture biases hidden behind graphs. Both  $\Delta SP$  and  $\Delta EO$  are highly model-dependent

and exhibit substantial variability even on the same dataset. For instance, GCN trained on German incurs significantly higher bias than other GNNs, whereas GraphSAGE trained on Pokec-z exhibits high bias for one sensitive attribute but much lower bias for the remaining attributes. These inconsistencies highlight the limitations of existing fairness metrics in the multi-attribute setting.

Due to the alignment between attribute privacy and group fairness [1, 27], Taipan can also serve as a fairness auditing to simultaneously infer multiple sensitive attributes, enabling the identification of both sensitive information leakage and structural group disparities.

**Table 7: Original Performance across Different Graph Datasets.** The red color indicates the commonly used sensitive attribute (SA) for fair or private graph learning, the arrow indicates the direction of better performance and the **bold font** represents the best results.

Dataset	GNN	AUC (↑)	ACC (↑)	F1 (↑)	SA1						SA2						SA3					
					$\Delta SP$ (↓)	$\Delta EO$ (↓)																
German	GCN	66.62	69.42	79.48	<b>21.37</b>	<b>13.50</b>	17.22	12.50	27.95	22.50												
	GraphSAGE	75.85	68.93	81.07	<b>3.67</b>	<b>0.50</b>	2.48	0.83	3.73	2.85												
	GIN	60.12	67.96	80.70	<b>0.47</b>	<b>1.50</b>	2.22	3.33	2.47	1.69												
Credit	GCN	71.86	75.22	83.93	0.98	15.73	<b>2.21</b>	<b>13.65</b>	—	—												
	GraphSAGE	73.40	79.55	87.81	1.50	0.42	<b>1.11</b>	<b>0.74</b>	—	—												
	GIN	73.73	78.98	87.54	0.95	1.27	1.68	<b>1.54</b>	—	—												
Pokec-n	GCN	60.91	64.43	57.24	5.46	10.73	<b>12.45</b>	<b>1.46</b>	74.12	32.32												
	GraphSAGE	62.18	65.34	57.38	1.35	5.90	<b>7.28</b>	<b>1.53</b>	73.07	32.52												
	GIN	60.36	64.60	56.90	2.28	13.58	<b>11.07</b>	<b>0.67</b>	67.13	33.52												
Pokec-z	GCN	64.92	59.52	51.86	9.33	12.60	<b>6.54</b>	<b>14.87</b>	81.70	33.33												
	GraphSAGE	66.55	59.13	54.41	69.80	101.56	<b>3.00</b>	<b>18.71</b>	79.42	5.74												
	GIN	65.61	60.64	53.46	44.43	61.06	<b>1.53</b>	<b>20.84</b>	88.50	27.66												

#### A.5 Visualization

**Embeddings of Multiple Sensitive Attributes** As illustrated in Figure 7, we utilize t-SNE to project the high-dimensional attack shared and task-specific node embeddings of multiple sensitive attributes into a two-dimensional space. We observe clear boundaries between shared and task-specific knowledge across all graphs, which indicates that Taipan successfully disentangles overlapping sensitive attributes into well-structured and identifiable clusters. Within most clusters, the original prototypes and their adjusted prototypes are located in close proximity to the corresponding cluster centers. The limited drift of the adapted prototypes from their original positions suggests that domain adaptation acts as a refinement process rather than a whole realignment, thereby avoiding overfitting to domain-specific noise. Furthermore, the embeddings on German exhibit more compact and well-separated patterns than those on other graphs, suggesting that Taipan can more effectively infer multiple sensitive attributes in this case. In addition, misclassified nodes primarily lie on the periphery or cluster boundaries. Intuitively, such boundary nodes typically have lower local homophily and generate more conflicting signals, which increasingly hinders G-MSAIAs.

**Joint Confidence Distributions** The joint confidence landscape of Taipan is further visualized in Figure 8. We observe a clear and dense high-confidence region where all sensitive

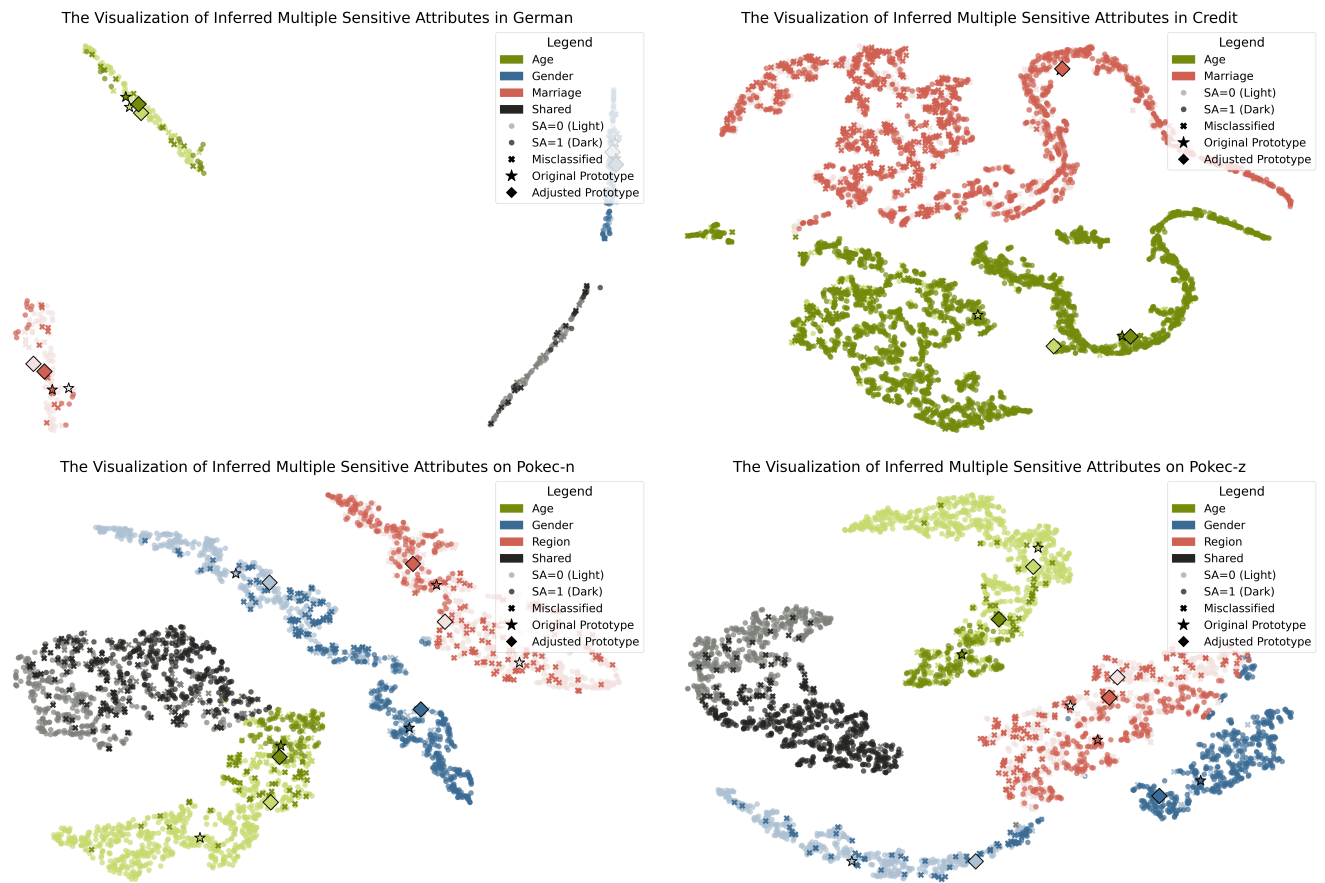


Figure 7: The tSNE Visualization of Inferred Multiple Sensitive Attributes

attributes are correctly inferred. In contrast, nodes with misclassified sensitive attributes are predominantly concentrated in low-confidence regions. Notably, nodes misclassified on only one sensitive attribute are not randomly distributed; instead, they cluster along the coordinate axes, where the attack model exhibits high confidence for one attribute but only moderate confidence for the other. This pattern reveals asymmetric and partial sensitive attribute leakage across different attack tasks. Overall, these observations indicate that Taipan’s internal confidence serves as a reliable proxy for G-MSAIAs.

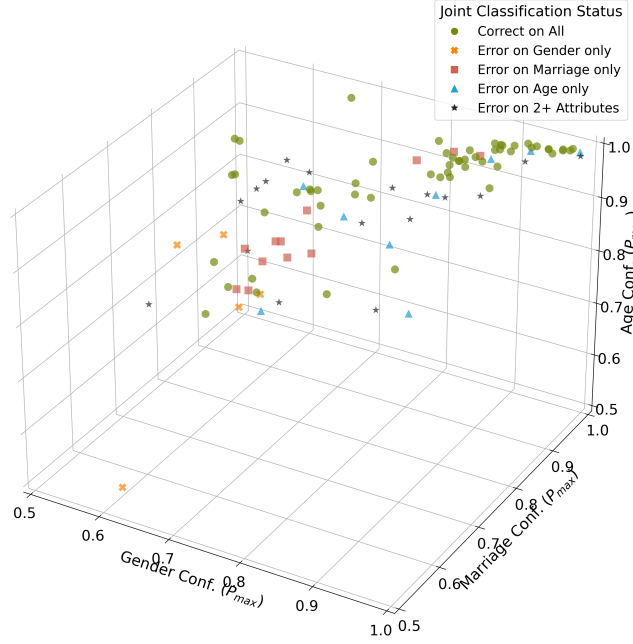
## A.6 Adaptation Steps

From Figure 9, SD generally increases as the number of adaptation steps grows, indicating that excessive adaptation gradually introduces semantic drift from the auxiliary graph. In contrast, within a small number of adaptation steps (e.g., fewer than 10), SD remains relatively low, suggesting a favorable trade-off between semantic preservation and computational costs. LC exhibits a comparatively stable trend across adaptation steps for most datasets. Although German shows mild oscillations as the number of steps increases, its overall performance remains stable, and better LC is consistently achieved within the first 10 adaptation steps. Taken together, these results suggest that a small number of adaptation steps is sufficient for G-MSAIAs.

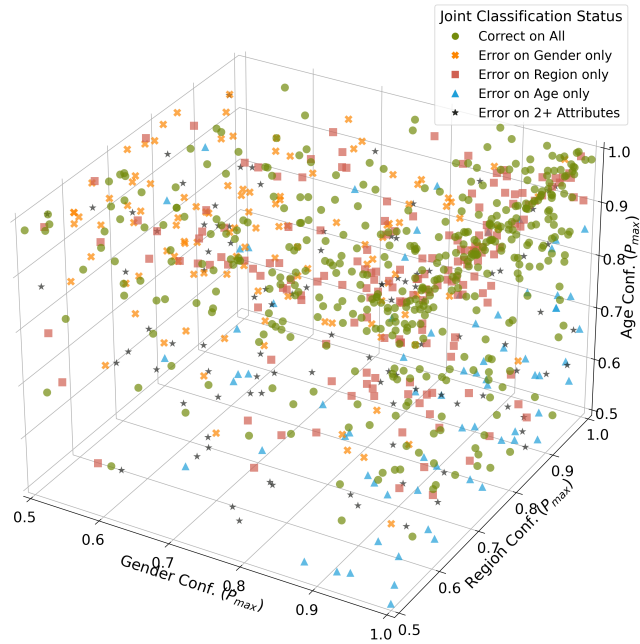
## A.7 Node Degree and Node Homophily

As shown in Figure 10, both node degree and node homophily exhibit clear correlations with per-node attack accuracy, particularly on German. Compared to subset accuracy, node-level attack accuracy exhibits more stable patterns. This difference is expected, as subset accuracy is an all-or-nothing metric that drops to zero once any sensitive attribute is incorrectly inferred, leading to more abrupt variations. In contrast, node-level accuracy captures partial privacy leakage, thereby providing a smoother view of attack effectiveness. Importantly, although some nodes attain zero subset accuracy, the majority of points stays consistently above 0.5, indicating that the adversary can still correctly infer a substantial fraction of sensitive attributes. This observation highlights that subset accuracy alone may underestimate privacy risks, as partial privacy leakage already constitutes a severe privacy threat.

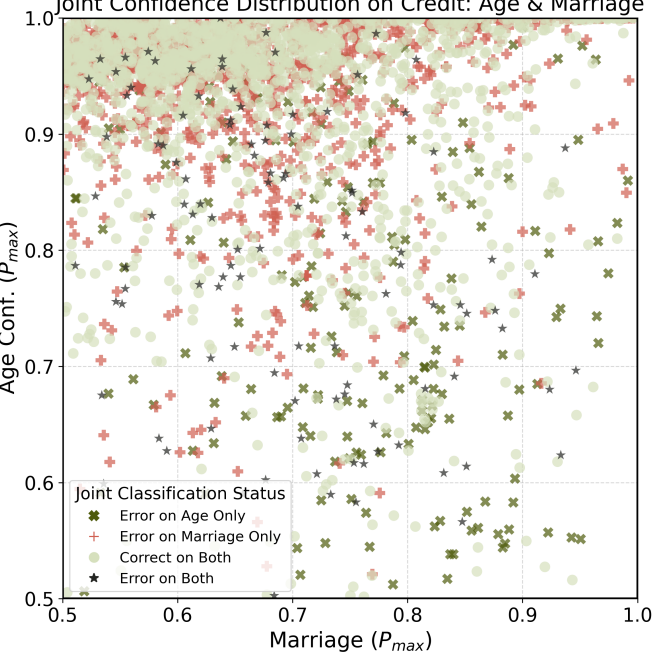
Joint Confidence Distribution on German: Gender (X) vs Marriage (Y) vs Age (Z)



Joint Confidence Distribution on Pokec-n: Gender (X) vs Region (Y) vs Age (Z)



Joint Confidence Distribution on Credit: Age & Marriage



Joint Confidence Distribution on Pokec-z: Gender (X) vs Region (Y) vs Age (Z)

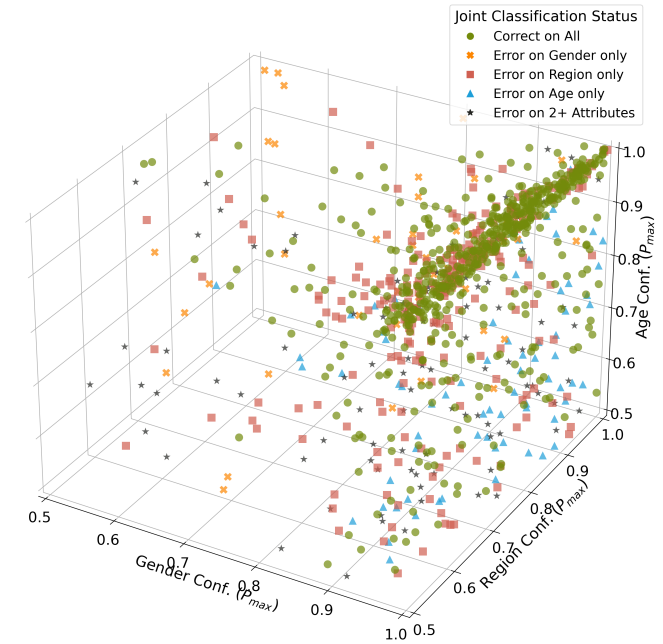


Figure 8: Joint Confidence Distribution for Multiple Sensitive Attributes

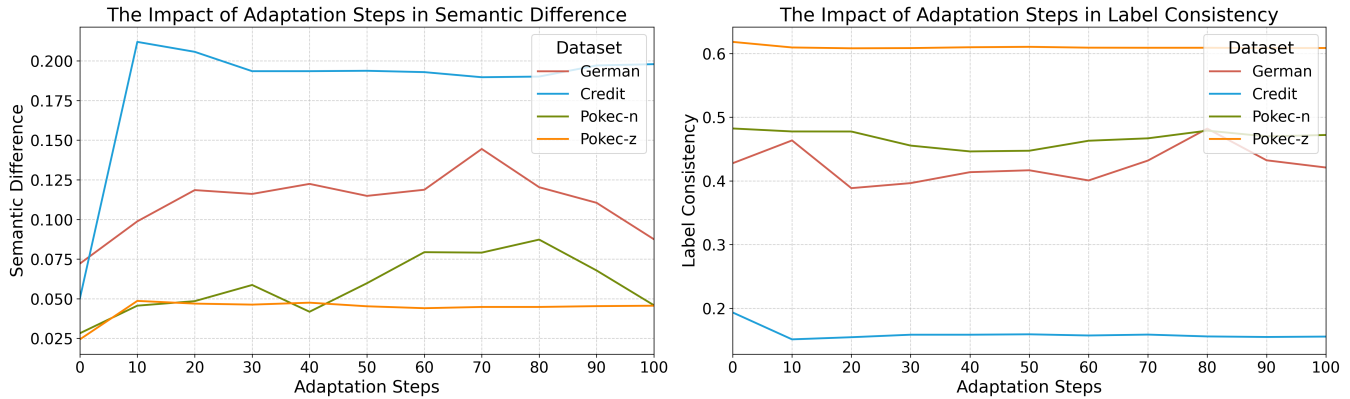


Figure 9: Impact of Adaptation Steps on Semantic-based Metrics

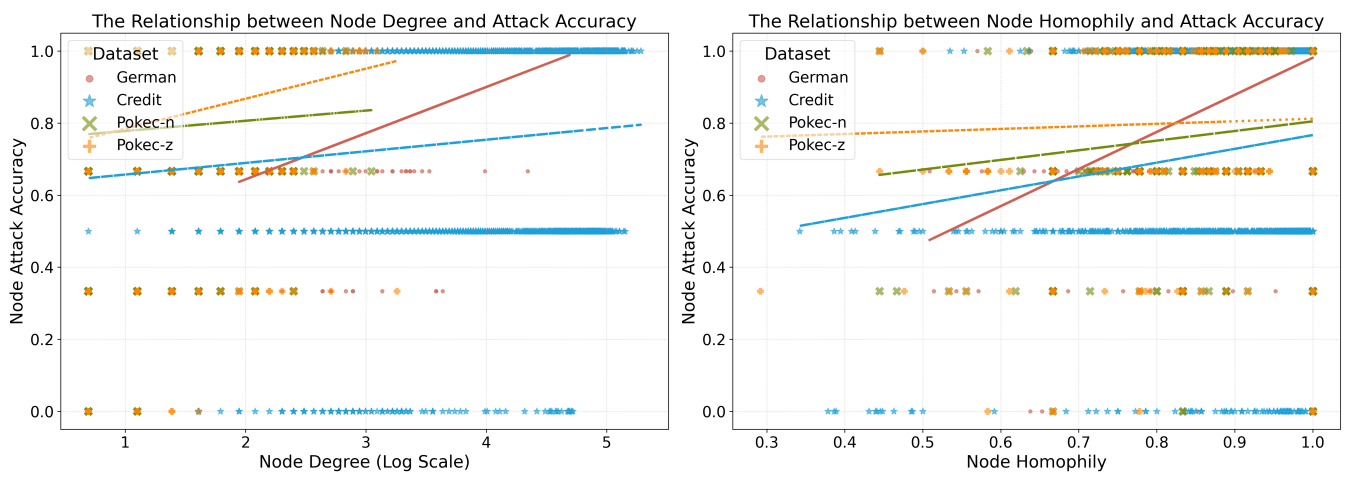


Figure 10: Impacts of Node Degree and Node Homophily on Attack Accuracy

## References

- [1] Jan Aalmoes, Vasisht Duddu, and Antoine Boutet. On the alignment of group fairness with attribute privacy. In Mahmoud Barhamgi, Hua Wang, and Xin Wang, editors, *Web Information Systems Engineering – WISE 2024*, pages 333–348, Singapore, 2025. Springer Nature Singapore.
- [2] Chirag Agarwal, Himabindu Lakkaraju, and Marinka Zitnik. Towards a unified framework for fair and stable graph representation learning. In Cassio de Campos and Marloes H. Maathuis, editors, *Proceedings of the Thirty-Seventh Conference on Uncertainty in Artificial Intelligence*, volume 161 of *Proceedings of Machine Learning Research*, pages 2114–2124. PMLR, 27–30 Jul 2021.
- [3] Peyman Baghershahi and Sourav Medya. Unsupervised prompting for graph neural networks. *arXiv preprint arXiv:2505.16903*, 2025.
- [4] Ting Bai, Le Huang, Yue Yu, Cheng Yang, Cheng Hou, Zhe Zhao, and Chuan Shi. Efficient multi-task prompt tuning for recommendation. *ACM Trans. Inf. Syst.*, 43(4), July 2025.
- [5] Yu Cao, Qian Wang, Xu Wang, Dezhong Peng, and Peilin Li. Multi-gate mixture of multi-view graph contrastive learning on electronic health record. *IEEE Journal of Biomedical and Health Informatics*, 29(6):3956–3967, 2025.
- [6] Qin Chen, Liang Wang, Bo Zheng, and Guojie Song. Dagprompt: Pushing the limits of graph prompting with a distribution-aware graph prompt tuning approach. In *Proceedings of the ACM on Web Conference 2025*, WWW ’25, page 4346–4358, New York, NY, USA, 2025. Association for Computing Machinery.
- [7] Wei Chen, Guo Ye, Yakun Wang, Zhao Zhang, Libang Zhang, Daixin Wang, Zhiqiang Zhang, and Fuzhen Zhuang. Smoothness really matters: a simple yet effective approach for unsupervised graph domain adaptation. In *Proceedings of the Thirty-Ninth AAAI Conference on Artificial Intelligence and Thirty-Seventh Conference on Innovative Applications of Artificial Intelligence and Fifteenth Symposium on Educational Advances in Artificial Intelligence, AAAI’25/IAAI’25/EAAI’25*. AAAI Press, 2025.
- [8] Djork-Arné Clevert, Thomas Unterthiner, and Sepp Hochreiter. Fast and accurate deep network learning by exponential linear units (elus). *arXiv preprint arXiv:1511.07289*, 4(5):11, 2015.
- [9] Enyan Dai and Suhang Wang. Say no to the discrimination: Learning fair graph neural networks with limited sensitive attribute information. In *Proceedings of the 14th ACM International Conference on Web Search and Data Mining*, WSDM ’21, page 680–688, New York, NY, USA, 2021. Association for Computing Machinery.
- [10] William H. E. Day and Herbert Edelsbrunner. Efficient algorithms for agglomerative hierarchical clustering methods. *Journal of Classification*, 1(1):7–24, December 1984.
- [11] Sayanton V. Dibbo, Dae Lim Chung, and Shagufta Mehnaz. Model inversion attack with least information and an in-depth analysis of its disparate vulnerability. In *2023 IEEE Conference on Secure and Trustworthy Machine Learning (SaTML)*, pages 119–135, 2023.
- [12] Vasisht Duddu, Antoine Boutet, and Virat Shejwalkar. Quantifying privacy leakage in graph embedding. In *MobiQuitous 2020 - 17th EAI International Conference on Mobile and Ubiquitous Systems: Computing, Networking and Services*, MobiQuitous ’20, page 76–85, New York, NY, USA, 2021. Association for Computing Machinery.
- [13] Matt Fredrikson, Somesh Jha, and Thomas Ristenpart. Model inversion attacks that exploit confidence information and basic countermeasures. In *Proceedings of the 22nd ACM SIGSAC Conference on Computer and Communications Security*, CCS ’15, page 1322–1333, New York, NY, USA, 2015. Association for Computing Machinery.
- [14] Tong Guan, Jiaheng Peng, and Jun Liang. Spatial-temporal graph multi-gate mixture-of-expert model for traffic prediction. In *2023 IEEE 26th International Conference on Intelligent Transportation Systems (ITSC)*, pages 36–41, 2023.
- [15] William L. Hamilton, Rex Ying, and Jure Leskovec. Inductive representation learning on large graphs. In *Proceedings of the 31st International Conference on Neural Information Processing Systems*, NIPS’17, page 1025–1035, Red Hook, NY, USA, 2017. Curran Associates Inc.
- [16] Kalle Hjerppe, Jukka Ruohonen, and Ville Leppanen. The general data protection regulation: Requirements, architectures, and constraints. In *2019 IEEE 27th International Requirements Engineering Conference (RE)*. IEEE, September 2019.
- [17] Bargav Jayaraman and David Evans. Are attribute inference attacks just imputation? In *Proceedings of the 2022 ACM SIGSAC Conference on Computer and Communications Security*, CCS ’22, page 1569–1582, New York, NY, USA, 2022. Association for Computing Machinery.

- [18] Ehsanul Kabir, Lucas Craig, and Shagufta Mehnaz. Disparate privacy vulnerability: Targeted attribute inference attacks and defenses. In *34th USENIX Security Symposium (USENIX Security 25)*. USENIX Association, August 2025.
- [19] Thomas N. Kipf and Max Welling. Semi-supervised classification with graph convolutional networks. In *International Conference on Learning Representations*, 2017.
- [20] Yajing Liu, Yuning Lu, Hao Liu, Yaozu An, Zhuoran Xu, Zhuokun Yao, Baofeng Zhang, Zhiwei Xiong, and Chenguang Gui. Hierarchical prompt learning for multi-task learning. In *2023 IEEE/CVF Conference on Computer Vision and Pattern Recognition (CVPR)*, pages 10888–10898, 2023.
- [21] Jiaqi Ma, Zhe Zhao, Xinyang Yi, Jilin Chen, Lichan Hong, and Ed H. Chi. Modeling task relationships in multi-task learning with multi-gate mixture-of-experts. In *Proceedings of the 24th ACM SIGKDD International Conference on Knowledge Discovery & Data Mining*, KDD ’18, page 1930–1939, New York, NY, USA, 2018. Association for Computing Machinery.
- [22] Shagufta Mehnaz, Sayanton V. Dibbo, Ehsanul Kabir, Ninghui Li, and Elisa Bertino. Are your sensitive attributes private? novel model inversion attribute inference attacks on classification models. In *31st USENIX Security Symposium (USENIX Security 22)*, pages 4579–4596, Boston, MA, August 2022. USENIX Association.
- [23] Daniel Morales-Brottons, Thijs Vogels, and Hadrien Hendrikx. Exponential moving average of weights in deep learning: Dynamics and benefits. *Transactions on Machine Learning Research*, 2024.
- [24] Chaoxi Niu, Guansong Pang, Ling Chen, and Bing Liu. Replay-and-forget-free graph class-incremental learning: A task profiling and prompting approach. In *The Thirty-eighth Annual Conference on Neural Information Processing Systems*, 2024.
- [25] Iyiola E. Olatunji, Anmar Hizber, Oliver Sihlovec, and Megha Khosla. Does black-box attribute inference attacks on graph neural networks constitute privacy risk?, 2023.
- [26] Iyiola E. Olatunji, Wolfgang Nejdl, and Megha Khosla. Membership inference attack on graph neural networks. In *2021 Third IEEE International Conference on Trust, Privacy and Security in Intelligent Systems and Applications (TPS-ISA)*, pages 11–20, 2021.
- [27] Ying Song and Balaji Palanisamy. Mapping: debiasing graph neural networks for fair node classification with limited sensitive information leakage. *World Wide Web*, 27(6):74, November 2024.
- [28] Mingchen Sun, Kaixiong Zhou, Xin He, Ying Wang, and Xin Wang. Gppt: Graph pre-training and prompt tuning to generalize graph neural networks. In *Proceedings of the 28th ACM SIGKDD Conference on Knowledge Discovery and Data Mining*, KDD ’22, page 1717–1727, New York, NY, USA, 2022. Association for Computing Machinery.
- [29] Xiangguo Sun, Hong Cheng, Jia Li, Bo Liu, and Jihong Guan. All in one: Multi-task prompting for graph neural networks. In *Proceedings of the 29th ACM SIGKDD Conference on Knowledge Discovery and Data Mining*, pages 2120–2131, 2023.
- [30] G’abor J. Sz’ekely, Maria L. Rizzo, and Nail K. Bakirov. Measuring and testing dependence by correlation of distances. *Annals of Statistics*, 35:2769–2794, 2007.
- [31] Lubos Takac and Michal Zabovsky. Data analysis in public social networks. In *International scientific conference and international workshop present day trends of innovations*, volume 1, 2012.
- [32] Huan Tian, Guangsheng Zhang, Bo Liu, Tianqing Zhu, Ming Ding, and Wanlei Zhou. Do fairness interventions come at the cost of privacy: Evaluations for binary classifiers. *IEEE Transactions on Dependable and Secure Computing*, 22:4654–4670, 2025.
- [33] Zichong Wang, Zhibo Chu, Thang Viet Doan, Shiwen Ni, Min Yang, and Wenbin Zhang. History, development, and principles of large language models: an introductory survey. *AI and Ethics*, 5(3):1955–1971, 2025.
- [34] Keyulu Xu, Weihua Hu, Jure Leskovec, and Stefanie Jegelka. How powerful are graph neural networks? In *International Conference on Learning Representations*, 2019.
- [35] Carl Yang, Haonan Wang, Ke Zhang, Liang Chen, and Lichao Sun. Secure deep graph generation with link differential privacy. In Zhi-Hua Zhou, editor, *Proceedings of the Thirtieth International Joint Conference on Artificial Intelligence, IJCAI-21*, pages 3271–3278. International Joint Conferences on Artificial Intelligence Organization, 8 2021. Main Track.
- [36] Jun Yu, Yutong Dai, Xiaokang Liu, Jin Huang, Yishan Shen, Ke Zhang, Rong Zhou, Eashan Adhikarla, Wenxuan Ye, Yixin Liu, Zhaoming Kong, Kai Zhang, Yilong Yin, Vinod Namboodiri, Brian D. Davison, Jason H. Moore, and Yong Chen. Unleashing the power of multi-task learning: A comprehensive survey spanning traditional, deep, and pretrained foundation model eras, 2024.

- [37] Xingtong Yu, Chang Zhou, Yuan Fang, and Xinming Zhang. Multigprompt for multi-task pre-training and prompting on graphs. In *Proceedings of the ACM Web Conference 2024, WWW '24*, page 515–526, New York, NY, USA, 2024. Association for Computing Machinery.
- [38] Quan Yuan, Zhikun Zhang, Linkang Du, Min Chen, Peng Cheng, and Mingyang Sun. PrivGraph: Differentially private graph data publication by exploiting community information. In *32nd USENIX Security Symposium (USENIX Security 23)*, pages 3241–3258, Anaheim, CA, August 2023. USENIX Association.
- [39] Ekim Yurtsever, Jacob Lambert, Alexander Carballo, and Kazuya Takeda. A survey of autonomous driving: Common practices and emerging technologies. *IEEE Access*, 8:58443–58469, 2020.
- [40] Boyang Zhang, Zheng Li, Ziqing Yang, Xinlei He, Michael Backes, Mario Fritz, and Yang Zhang. SecurityNet: Assessing machine learning vulnerabilities on public models. In *33rd USENIX Security Symposium (USENIX Security 24)*, pages 3873–3890, Philadelphia, PA, August 2024. USENIX Association.
- [41] Cong Zhang, Dongyang Liu, Lin Zuo, Junlan Feng, Chao Deng, Jian Sun, Haitao Zeng, and Yaohong Zhao. Multi-gate mixture-of-contrastive-experts with graph-based gating mechanism for tv recommendation. In *Proceedings of the 32nd ACM International Conference on Information and Knowledge Management, CIKM '23*, page 4938–4944, New York, NY, USA, 2023. Association for Computing Machinery.
- [42] Sen Zhang, Haibo Hu, Qingqing Ye, and Jianliang Xu. Privedpr: Synthetic graph publishing with deep pagerank under differential privacy. In *Proceedings of the 31st ACM SIGKDD Conference on Knowledge Discovery and Data Mining V.1*, KDD '25, page 1936–1947, New York, NY, USA, 2025. Association for Computing Machinery.
- [43] Zhikun Zhang, Min Chen, Michael Backes, Yun Shen, and Yang Zhang. Inference attacks against graph neural networks. In *31st USENIX Security Symposium (USENIX Security 22)*, pages 4543–4560, Boston, MA, August 2022. USENIX Association.
- [44] Benjamin Zi Hao Zhao, Aviral Agrawal, Catisha Coburn, Hassan Jameel Asghar, Raghav Bhaskar, Mohamed Ali Kaafar, Darren Webb, and Peter Dickinson. On the (in)feasibility of attribute inference attacks on machine learning models. In *2021 IEEE European Symposium on Security and Privacy (EuroS&P)*, pages 232–251, 2021.